Published in final edited form as:
Mol Microbiol. 2014 August ; 93(4): 759–775. doi:10.1111/mmi.12693.

The *Yersinia pestis* Siderophore, Yersiniabactin, and the ZnuABC system both contribute to Zinc acquisition and the development of lethal septicemic plague in mice

Alexander G. Bobrov[a], **Olga Kirillina**[a], **Jacqueline D. Fetherston**[a], **M. Clarke Miller**[b,*], **Joseph A. Burlison**[b], and **Robert D. Perry**[a,‡]

[a]Department of Microbiology, Immunology, and Molecular Genetics, University of Kentucky, Lexington, KY

[b]James Graham Brown Cancer Center, University of Louisville, Louisville, KY

Summary

Bacterial pathogens must overcome host sequestration of zinc (Zn^{2+}), an essential micronutrient, during the infectious disease process. While the mechanisms to acquire chelated Zn^{2+} by bacteria are largely undefined, many pathogens rely upon the ZnuABC family of ABC transporters. Here we show that in *Yersinia pestis*, *irp2*, a gene encoding the synthetase (HMWP2) for the siderophore yersiniabactin (Ybt) is required for growth under Zn^{2+}-deficient conditions in a strain lacking ZnuABC. Moreover, growth stimulation with exogenous, purified apo-Ybt provides evidence that Ybt may serve as a zincophore for Zn^{2+} acquisition. Studies with the Zn^{2+}-dependent transcriptional reporter *znuA*::*lacZ* indicate that the ability to synthesize Ybt affects the levels of intracellular Zn^{2+}. However, the outer membrane receptor Psn and TonB as well as the inner membrane (IM) ABC transporter YbtPQ, that are required for Fe^{3+} acquisition by Ybt, are not needed for Ybt-dependent Zn^{2+} uptake. In contrast, the predicted IM protein YbtX, a member of the Major Facilitator Superfamily, was essential for Ybt-dependent Zn^{2+} uptake. Finally, we show that the ZnuABC system and the Ybt synthetase HMWP2, presumably by Ybt synthesis, both contribute to the development of a lethal infection in a septicemic plague mouse model.

Introduction

Zinc (Zn^{2+}) is an essential trace metal which has structural and/or catalytic functions in an estimated 3-8% of bacterial proteins (Andreini *et al.*, 2006; Hantke, 2005; Katayama *et al.*, 2002; Vallee and Falchuk, 1993). Similar to iron, mammalian hosts restrict the availability of Zn^{2+} to invading pathogens by a number of mechanisms. Zn^{2+} serum levels are in the micromolar range with the metal tightly chelated by proteins such as transferrin, albumin and α_2-macrogloubin (Foote and Delves, 1984; Rahuel-Claremont and Dunn, 1998; Rink and Haase, 2007; Weinberg, 1972). Upon infection, mammals sequester Zn^{2+} systemically and locally in an attempt to further reduce access to this critical micronutrient; one example

‡For correspondence. rperry@uky.edu; Tel (+1) 859 323-6341; Fax (+1) 859 257 8994.
*Current address: Department of Chemistry and Biochemistry, University of North Georgia, Gainesville, GA

The authors have no conflicts of interest to declare.

being calprotectin (Corbin *et al.*, 2008; Foote and Delves, 1984; Hood and Skaar, 2012; Kehl-Fie and Skaar, 2010; Liuzzi *et al.*, 2005; Rahuel-Claremont and Dunn, 1998; Rink and Haase, 2007; Sohnle *et al.*, 2000; Weinberg, 1972). Consequently high affinity Zn^{2+} uptake systems should be needed to acquire this transition metal during the infectious process.

In contrast to the variety of bacterial iron uptake systems, relatively few bacterial high-affinity Zn^{2+} uptake systems have been identified. The ABC transporter ZnuABC (and its cluster 9 [C9] family orthologs) remains the most widespread mechanism for high affinity Zn^{2+} uptake. In some bacteria, a second periplasmic Zn^{2+}-binding protein, ZinT, works in conjunction with ZnuA, the primary periplasmic Zn^{2+}-binding protein of the ZnuABC system (Graham *et al.*, 2009; Hantke, 2005; Kehl-Fie and Skaar, 2010; Petrarca *et al.*, 2010). ZupT, a member of the ZIP family of proton motive force-dependent transporters, is described as a low-affinity Zn^{2+} transporter but contributes to Zn^{2+} uptake at a concentration of 10 μM Zn^{2+} *in vitro*, and in infection models, at least for *E. coli* UPEC and *Salmonella* (Cerasi *et al.*, 2014; Grass *et al.*, 2002; Karlinsey *et al.*, 2010; Sabri *et al.*, 2009). Additional inner membrane (IM) transporters ZevAB and ZurAM have recently been implicated in Zn^{2+} acquisition by *Haemophilus influenzae* and *Listeria monocytogenes*, respectively (Corbett *et al.*, 2012; Rosadini *et al.*, 2011).

Little is known about Zn^{2+} transport across the outer membrane (OM). In *Neisseria meningitidis*, a TonB-dependent OM receptor (ZnuD), with high similarity to heme OM receptors, functions in zinc and heme uptake (Kumar *et al.*, 2012; Stork *et al.*, 2010). In *Acinetobacter baumannii*, two genes encoding TonB-dependent OM receptors with similarities to ZnuD are repressed by Zn^{2+} (Hood *et al.*, 2012). The cyanobacterium *Anabaena* encodes two TonB-dependent OM receptors whose transcription is highly repressed by the Zn^{2+}-responsive transcriptional regulator Zur (Napolitano *et al.*, 2012). However the substrate(s) for these receptors has not been investigated.

Secreted Zn^{2+}-chelating compounds (zincophores), analogous to siderophores which chelate Fe^{3+}, have been proposed as a Zn^{2+} acquisition mechanism for pathogens (Hood and Skaar, 2012) and confirmed in several organisms. The fungal pathogen *Candida albicans* secretes an ∼33 kDa Zn^{2+}-binding protein, Pra1, involved in Zn^{2+} scavenging (Citiulo *et al.*, 2012). *Pseudomonas putida* produces a small siderophore (198 daltons), pyridine-2,6-bis(thiocarboxylic acid) (PDTC), that binds Fe^{3+} and Zn^{2+} and delivers these cations to the bacterial cell (Cortese *et al.*, 2002; Leach *et al.*, 2007). Finally, *Streptomyces coelicolor* produces a siderophore-like molecule, coelibactin, which has been proposed, but not proven, as a zincophore (Hesketh *et al.*, 2009; Zhao *et al.*, 2012).

A role for Zn^{2+} acquisition during infections has been demonstrated in a number of bacterial pathogens: *Acinetobacter baumannii, Brucella abortus, Campylobacter jejuni*, pathogenic *E. coli* strains, *Haemophilus ducreyi, H. influenzae, L. monocytogenes, Moraxella catarrhalis, Neisseria gonorrhoeae, Pasteurella multocida, Proteus mirabilis, Salmonella enterica* serovar Typhimurium, *Streptococcus pneumoniae, Streptococcus pyogenes, Vibrio parahaemolyticus*, and *Yersinia ruckeri* (Ammendola *et al.*, 2007; Bayle *et al.*, 2011; Campoy *et al.*, 2002; Cerasi *et al.*, 2013; Cerasi *et al.*, 2014; Corbett *et al.*, 2012; Dahiya and Stevenson, 2010; Davis *et al.*, 2009; Gabbianelli *et al.*, 2011; Garrido *et al.*, 2003; Hood *et*

al., 2012; Karlinsey *et al.*, 2010; Kim *et al.*, 2004; Lewis *et al.*, 1999; Lim *et al.*, 2008; Liu *et al.*, 2012; Liu *et al.*, 2013; Murphy *et al.*, 2013; Nielubowicz *et al.*, 2010; Plumptre *et al.*, 2014; Rosadini *et al.*, 2011; Sabri *et al.*, 2009; Weston *et al.*, 2009; Yang *et al.*, 2006).

Yersinia pestis is a Gram-negative bacterium that causes a flea-borne zoonotic disease, bubonic plague. After the infected flea bite, *Y. pestis* typically spreads from the site of the mammalian skin wound to the regional lymph node where multiplying bacteria cause necrosis resulting in a swollen and painful lymph node or bubo. Bubonic plague progresses rapidly to an often terminal systemic stage of disease or septicemic plague. A small proportion of mammals can develop septicemia without a prior lymphatic stage when plague bacteria are directly injected into the blood vessel by the flea bite or other means. Septicemia is required to infect naïve fleas, completing the zoonotic disease cycle. During the course of mammalian disease, the lungs may become infected leading to the development of secondary pneumonic plague. In humans that have developed secondary pneumonic plague, *Y. pestis* can then spread via respiratory droplets from person to person causing primary pneumonic plague (Perry and Fetherston, 1997; Sebbane *et al.*, 2010; Sebbane *et al.*, 2006).

We previously showed that ZnuABC is required during *in vitro* growth of *Y. pestis* in Chelex-100-treated PMH2 medium (cPMH2) which contains submicromolar Zn^{2+} levels (Desrosiers *et al.*, 2010; Perry *et al.*, 2012). Both the *znuA* and *znuCB* promoters are regulated by Zn^{2+} via the transcriptional regulator Zur that is common to many bacteria; a mutation in the *Y. pestis znu* system increases expression under low Zn^{2+} conditions. However, the growth response of the *Y. pestis znu* mutant to supplementation of cPMH2 with 0.4 μM $ZnCl_2$, suggests that *Y. pestis* has a second high-affinity Zn^{2+} transporter. In addition, the *znu* mutant is highly virulent in mouse models of bubonic and pneumonic plague lending further support to the existence of another unidentified *Y. pestis* Zn^{2+} transporter that can effectively substitute for ZnuABC during mammalian infections. Deletion or overexpression of nine genetic loci that encode divalent cation transporters or cation transporters repressed by Zn^{2+} -Zur showed that none of these systems are needed by a *znu* mutant for *in vitro* growth under Zn^{2+} -deficient conditions (Desrosiers *et al.*, 2010; Li *et al.*, 2009; Perry *et al.*, 2012). Thus one or more Zn^{2+} transporters of *Y. pestis* remained to be identified.

Siderophores are low-molecular weight compounds produced and secreted by bacteria, fungi and plants and are typically associated with the chelation of ferric iron (Fe^{3+}) for acquisition by the producing organism. Siderophores are often vital for bacteria in different environments, including the mammalian host where some can remove iron from lactoferrin and transferrin (Hood and Skaar, 2012; Schaible and Kaufmann, 2004). While siderophores have a high affinity for Fe^{3+}, some, including pyochelin which is structurally similar to the yersiniabactin (Ybt) siderophore produced by *Yersinia* and other bacteria (Fig. 1), have been shown to bind other transition metals as well (Braud *et al.*, 2010; Braud *et al.*, 2009a; Braud *et al.*, 2009b; Chaturvedi *et al.*, 2012). In addition, micacocidin, a compound with a chemical structure similar to Ybt made by *Pseudomonas* spp and *Ralstonia solanacearum* (Fig. 1), has been crystallized with Zn^{2+}, Mn^{2+}, and Fe^{3+} (Kreutzer *et al.*, 2011; Nakai *et al.*,

1999). However, there is no evidence that siderophore-dependent acquisition of transition metals other than iron plays any role in bacterial pathogenesis.

In *Y. pestis*, the Ybt siderophore-dependent iron uptake system has been shown to have a primary role in iron acquisition *in vitro* and to be essential for the development of bubonic plague and critical in pneumonic plague (Fetherston *et al.*, 2010; Perry and Fetherston, 2011). Iron uptake via the Ybt system requires the TonB-dependent OM receptor Psn, TonB and the IM ABC transporter YbtPQ (Fetherston *et al.*, 1999; Fetherston *et al.*, 1995; Perry *et al.*, 2003b) Here, we demonstrate that the Ybt siderophore and the IM protein YbtX play a role in Zn^{2+} accumulation and that both ZnuABC and Ybt synthetase HMWP2 are critical for lethal infections in a mouse model of septicemic plague.

Results

The *pgm* locus that encodes the Ybt system is required for growth under metal-deficient conditions and for the virulence of a *znu* mutant

Previously we failed to identify a putative second Zn^{2+} uptake system that allowed Zn^{2+} use from low concentrations *in vitro* and full virulence of a *Y. pestis znu* mutant (Desrosiers *et al.*, 2010; Perry *et al.*, 2012). Since then two previously unknown bacterial Zn^{2+} transporters, ZurAM (not encoded in *Y. pestis*) and ZevAB, have been shown to be important for Zn^{2+} uptake and virulence by *L. monocytogenes* and *H. influenzae*, respectively (Corbett *et al.*, 2012; Rosadini *et al.*, 2011). Y1329-1330 are ZevAB homologues encoded in *Y. pestis* KIM10+. Y1329 and ZevA each have a COG3683 domain which is annotated as a periplasmic component of an ABC transporter. Like *H. influenza zevB* and the *Y. pestis* Zn^{2+}-repressible *y1245* gene (Li *et al.*, 2009), *y1330* encodes a NicO domain that is annotated as a proton motive force-dependent nickel transport permease. While some NicO domain proteins have demonstrated Ni^{2+} uptake activity, including the Y1245 homolog in *Yersinia pseudotuberculosis* (Sebbane *et al.*, 2002), the evidence in *H. influenzae* suggests they may also participate in Zn^{2+} transport (Rosadini *et al.*, 2011). Previously, we showed that a *znu y1245* double mutant grew as well as a *znu* mutant in cPMH2 medium (Desrosiers *et al.*, 2010). Since Y1245 and Y1330 might serve redundant Zn^{2+} uptake functions, we constructed and tested a Δ*znuBC* Δ*y1245*::*cam* Δ*y1329-y1330*::*kan* triple mutant. Growth of the Δ*znuBC* single mutant and the triple mutant at 37°C did not differ significantly in cPMH2 with or without $ZnCl_2$ added to 0.6 μM (Fig. S1in supporting information). Thus neither of these NicO domain proteins nor Y1329 appears to play a critical role in Zn^{2+} uptake in *Y. pestis.*

We noted that the Ybt siderophore, which has a high affinity for Fe^{3+} vs ferrous (Fe^{2+}) iron, has recently been shown to chelate Cu^{2+} (Chaturvedi *et al.*, 2012; Perry *et al.*, 1999) and that the structurally similar micacocidin (Fig. 1A) has been crystallized with Zn^{2+} (Kreutzer *et al.*, 2011; Nakai *et al.*, 1999). Therefore, we hypothesized that the Ybt system might be involved in Zn^{2+} uptake with the Ybt siderophore serving as a zincophore. In preliminary studies, we used *Y. pestis* KIM6 strains with a spontaneous deletion of the chromosomal *pgm* locus that eliminates four *ybt* operons encoding siderophore biosynthetic, uptake, and regulatory functions (Bearden *et al.*, 1997; Fetherston and Perry, 1994; Perry and Fetherston, 2011). Strikingly, we found that a combination of *pgm* and *znuBC* deletions

completely abrogated growth of this mutant in cPMH2 supplemented with 0.6 μM $ZnCl_2$ compared to the parent Pgm^+ Δ*znuB*C mutant (Fig. 2A). This growth defect was rescued by integration of the *znuA* and *znuCB* operons into the *att* Tn*7* site on the chromosome of the double Δ*pgm* Δ*znuBC* mutant (data not shown). Thus, it appears that gene(s) within the *pgm* locus are involved in Zn^{2+} acquisition by *Y. pestis*.

A *Y. pestis* KIM Δ*pgm* mutant is completely avirulent by subcutaneous injection (bubonic plague) and highly attenuated by intranasal installation (pneumonic plague). However, various *Y. pestis* Δ*pgm* strains, including KIM, are fully virulent via an intravenous route of infection (septicemic plague) (Bearden and Perry, 1999; Fetherston *et al.*, 2010; Jackson and Burrows, 1956; Une and Brubaker, 1984). Consequently, we used a mouse model of septicemic plague to compare Δ*pgm* and Δ*pgm* Δ*znuBC* mutants. Unlike our *in vitro* studies, these strains carry pCD1Ap, a plasmid encoding a type three secretion system and effector proteins that is essential for virulence (Gong *et al.*, 2001; Perry *et al.*, 1998). The Δ*pgm* Δ*znuBC* mutant had an $\sim 10^6$-fold loss of virulence compared to the Δ*pgm* strain. The virulence of the Δ*pgm* Δ*znuBC* mutant was restored by complementation with the $znuABC^+$ locus integrated into the chromosome (Table 1). A time-to-death analysis comparing these three strains (Δ*pgm*, Δ*pgm* Δ*znuBC*, Δ*pgm* $znuBC^{-/+}$) strikingly illustrates these virulence differences (Fig. 2B). Thus, the Zn^{2+} uptake system, ZnuABC, and components within the *pgm* locus are critical for the development of lethal infection in a mouse model of septicemic plague.

The *irp2* gene, encoding the Ybt synthase HMWP2, is involved in Zn^{2+} acquisition

To specifically address the role of the Ybt system in Zn^{2+} acquisition, we constructed an *irp2*::*kan* mutation in the Δ*znuBC* strain. The *irp2*-encoded HMWP2 protein is essential for the synthesis of Ybt – condensing two cysteines and linking them to salicylate to form three of the first four heterocylic rings of Ybt (Fig. 1A) (Perry and Fetherston, 2011). We previously demonstrated that the *kan* insertion in *irp2* has a polar effect on downstream genes in the *irp2-irp1-ybtUTE* operon, completely abrogating Ybt biosynthesis (Bearden *et al.*, 1997; Miller *et al.*, 2010; Perry *et al.*, 1999). For growth studies of this mutant, cPMH2 was supplemented with 1 μM $FeCl_3$ and 0.6 μM $ZnCl_2$. Iron was added to compensate for the loss of iron uptake via the Ybt system while submicromolar Zn^{2+} was added to enhance the growth of the single Δ*znuBC* mutant. This single mutant showed the expected growth defect compared to the Ybt^+ Znu^+ parent strain while the *irp2*::*kan* Δ*znuBC* double mutant exhibited no growth in cPMH2 despite $FeCl_3$ and $ZnCl_2$ supplementation (Fig. 3A). Moreover, a similar severe growth defect was caused by an in-frame deletion of *irp2* in the Δ*znuBC* background. This defect was alleviated by complementation of the Δ*irp2* mutation with a plasmid expressing the cloned *irp2* gene (Fig. 3B). Thus, our data indicate that, in addition to Zn^{2+} uptake by the ZnuABC system, the Ybt system is needed for *Y. pestis* growth under low Zn^{2+} conditions in the absence of ZnuABC and that Ybt may serve as a zincophore.

Our original Δ*znuBC* mutation eliminates the entire *znuC* ORF, most of *znuB* and the promoter regions between *znuA* and *znuCB* (Desrosiers *et al.*, 2010). The *y2248* gene that encodes a member of the M23 family of endopeptidases lies only 20 bp downstream of *znuA*

(Fig. S2). Thus, it is possible that *znuA* and *y2248* are transcribed from the same promoter, in which case the expression of *y2248* would be abrogated in the *znuBC* mutant. Consequently, we constructed an in-frame *znuA* deletion (Fig. S2) in KIM6+ and the Δ*irp2* mutant and tested their growth under low Zn^{2+} conditions. Both the Δ*znuA* and Δ*irp2* Δ*znuA* mutants had identical *in vitro* and *in vivo* phenotypes compared to the Δ*znuBC* and Δ*irp2* Δ*znuBC* mutants, respectively (data not shown; Table 1). These data together with the results showing that the Δ*znuBC* mutation is complemented by integration of *znuABC*$^{+}$ into the *att* Tn*7* site confirm that the *znuBC* mutation is responsible for the *Y. pestis* growth defect under *in vitro* low Zn^{2+} conditions.

The intracellular levels of Zn^{2+} in *Y. pestis* and other bacteria are tightly regulated by the Zn^{2+}-responsive transcriptional regulator Zur that represses *znuA* and *znuCB* promoters under Zn^{2+}-sufficient conditions (Desrosiers *et al.*, 2010; Hantke, 2005; Li *et al.*, 2009). Using a *znuA*::*lacZ* reporter we have previously shown that transcription from the *znuA* promoter during growth in cPMH2 in the Δ*znuBC* mutant is higher than in the parent Znu^{+} strain (Desrosiers *et al.*, 2010). We used the same reporter to determine whether the Ybt system plays any role in Zn^{2+} acquisition when ZnuABC is functional. In the single *irp2*::*kan* mutant, growth in unsupplemented cPMH2 showed a significant (∼2-fold) increase in transcription from *znuA*::*lacZ* compared to the Ybt^{+} parent strain (Fig. 4A). Thus the Ybt system contributes to intracellular Zn^{2+} levels even when ZnuABC is functional.

We again used the *znuA*::*lacZ* reporter to determine if the double *irp2*::*kan* Δ*znuBC* mutant is more Zn^{2+} starved than the single Δ*znuBC* mutant. In the single mutant, 10 μM $ZnCl_2$ caused a 5-fold loss of β-galactosidase activity from *znuA*::*lacZ* compared with 0.6 μM $ZnCl_2$ while the double *irp2*::*kan* Δ*znuBC* mutant showed only a 1.3-fold loss of β-galactosidase activity under the same growth conditions. At 10 μM $ZnCl_2$, *znuA*::*lacZ* activity in the single mutant was repressed 4.7-fold compared to the double mutant (Fig. 4B). These data indicate that the Ybt system supplies Zn^{2+} that represses the *znuA*::*lacZ* reporter under these growth conditions.

These differences in intracellular Zn^{2+} levels due to loss of uptake functions translate into growth defects. Zn^{2+} titration studies demonstrated that the Δ*znuBC* mutant in cPMH2 with 0.6 μM $ZnCl_2$ grew as well as the *irp2*::*kan* Δ*znuBC* mutant only when the double mutant was grown with 2.5 μM $ZnCl_2$ (Fig. 4C). In addition, supplementation of cPMH2 with 0.6 μM $ZnCl_2$ and 10 μM $FeCl_3$ showed no alleviation of the growth defect (Fig. 4C). Thus, our data confirm that growth of the double mutant is Zn^{2+}-dependent and not iron-dependent.

Expression of HMWP2 from the *irp2-irp1-ybtUTE* promoter is normally repressed by iron (Perry *et al.*, 2003a), to determine if it is also affected by Zn^{2+} we examined the activity of an *irp2*::*lacZ* transcriptional reporter (pEUIrp2) in Ybt^{+} Znu^{+} and Ybt^{+} Znu^{-} strains. Cells were grown in cPMH with or without $ZnCl_2$ or $FeCl_3$ added to 10μM. In a Znu^{+} background, transcription of the *irp2* promoter was repressed by iron but not by Zn^{2+} (Fig. 5). This is in agreement with the microarray finding of Li *et al* that *ybt* operons are not regulated by Zn^{2+} or Zur (Li *et al.*, 2009). However, the *znu* mutation resulted in an ∼1.7 fold increase in transcription from the *irp2* promoter compared to the Znu^{+} parent, which was repressed by Zn^{2+} (∼1.6-fold) as well as Fe^{3+} (Fig.5). Iron repressed transcription of

the *irp2* reporter ~10-12 fold in a Znu^+ background but only ~4 fold in the Znu^- strain. These results show that extreme Zn^{2+} starvation can affect expression of the Ybt system; perhaps, the low intracellular Zn^{2+} levels affect Fur activity. At least *in vitro*, *E. coli* and *Bacillus subtilis* Fur proteins bind Fe^{2+} as well as other divalent metals, including Zn^{2+}. In addition, Fur has been shown to bind Zn^{2+} as a structural component (Althaus *et al.*, 1999; Ma *et al.*, 2012; Mills and Marletta, 2005; Sheikh and Taylor, 2009). Perhaps, in the *znu* mutant, there is insufficient Zn^{2+} for maximal Fur activity. Thus, in the absence of Zn^{2+} the *irp2*::*lacZ* reporter is not fully repressed in this strain. The finding that the activity of this reporter in the presence of Zn^{2+} is the same in both Znu^+ and Znu^- strains lends credence to this hypothesis.

TonB-dependent OM receptors are not required for Zn^{2+} acquisition in *Y. pestis*

The OM receptor Psn is required for Fe^{3+} acquisition by the Ybt siderophore and its function is dependent upon TonB, an IM anchored, periplasm spanning protein that is required for active transport across the OM via TonB-dependent receptors. *Y. pestis* strains with mutations in either *psn* or *tonB* exhibit a severe growth defect due to increased chelation of residual Fe^{3+} from the medium by Ybt that is unable to enter the cells. These growth defects can be rescued by supplementation with 1μM $FeCl_3$. *Y. pestis* has a second TonB-like gene (*hasB*) that is not required for Fe^{3+}-Ybt utilization (Fetherston *et al.*, 1995; Perry *et al.*, 2003b; Perry and Fetherston, 2011).

In *Pseudomonas* species, TonB-dependent receptors required for Fe^{3+}-siderophore uptake are also needed for the uptake of siderophores complexed with other metals (Braud *et al.*, 2010; Hannauer *et al.*, 2012; Leach *et al.*, 2007; Schalk *et al.*, 2011). To test if the Psn receptor is also involved in Zn^{2+} acquisition via Ybt, we constructed either Δ*psn* or Δ*psn*::*kan* mutations in the Znu^- strain. Surprisingly, in contrast to the Δ*irp2* Δ*znuBC* and *irp2*::*kan* Δ*znuBC* double mutants, both the Δ*psn* Δ*znuBC* and Δ*psn*::*kan* Δ*znuBC* mutants grew as well as the Δ*znuBC* and *psn* single mutants in cPMH2 supplemented with 1.0 μM $FeCl_3$ and 0.6 μM $ZnCl_2$ (Fig. 6A). Curiously, the Δ*psn*::*kan* Δ*znuBC* strain grew better than the Δ*znu* mutant when Zn^{2+} was omitted from the growth medium (Fig. 6A), suggesting that the Psn receptor might hinder Ybt-dependent Zn^{2+} uptake in *Y. pestis*.

While these results suggest that Ybt synthesized by HMWP2 provides Zn^{2+} by a route independent of the Fe^{3+}-Ybt uptake system, a different OM receptor might be used for Zn^{2+} uptake. *Y. pestis* has a second locus encoding Ybt-like proteins with Y3404 showing significant similarity to Psn (21% identity and 39% similarity) (Forman *et al.*, 2010; Perry and Fetherston, 2004). In addition, the TonB-dependent OM receptor ZnuD in *Neisseria meningitidis* has similarities to the family of heme receptors and functions in heme and Zn^{2+} uptake (Kumar *et al.*, 2012; Stork *et al.*, 2010). To determine if TonB is required for Zn^{2+} acquisition, we constructed a mutant lacking both of the *Y. pestis tonB* genes in a Δ*znuBC* background. Again, the Δ*tonB*::*kan* Δ*hasB* Δ*znuBC* and single Δ*znuBC* mutants had similar growth defects in cPMH2 supplemented with 1.0 μM $FeCl_3$ and 0.6 μM $ZnCl_2$ (Fig. 6B). This indicates that Ybt-dependent Zn^{2+} uptake does not require any TonB-dependent OM receptor in *Y. pestis*.

The Ybt synthetase but not the Ybt OM receptor is critical for virulence in a Znu$^-$ background during septicemic plague

Based on studies using *Y. pestis* Δ*pgm* strains, it is clear that the Ybt system is not essential for the virulence of *Y. pestis* by an intravenous route of infection (Bearden and Perry, 1999; Jackson and Burrows, 1956; Une and Brubaker, 1984). However, specific mutations in *ybt* genes have not been tested in a mouse model of septicemic plague. LD_{50}s for the Ybt$^+$ strain as well as the Δ*psn*::*kan* and *irp2*::*kan* mutants were similar and confirm that *Y. pestis* does not require the Ybt system to cause lethal septicemic plague in mice (Table 1).

However, the *irp2*::*kan* mutant, which had an LD_{50} similar to that of the Ybt$^+$ parent strain, showed some attenuation at low infectious doses. While all 8 mice infected with the parent strain at infectious doses of 13 and 15 quickly succumbed to infection, 5 out 8 mice infected with doses of 11 and 16 cells of the *irp2*::*kan* mutant survived ($p = 0.01$). Thus, while the Ybt system is not required for septicemic plague it may play a modest role during the systemic stage of the infection resulting from low infectious doses.

To assess the importance of the Ybt-dependent Zn^{2+} acquisition during septicemic plague, we tested the effect of *irp2* mutations in Δ*znu* backgrounds. All three double mutants, Δ*irp2* Δ*znuBC*, *irp2*::*kan* Δ*znuBC*, Δ*irp2* Δ*znuA*, showed drastic attenuation ($\sim 10^5$-fold virulence losses) compared to the Ybt$^+$ Znu$^+$ parent strain as well as single Δ*znuBC* and *znuA* mutants (Table 1). Thus HMWP2 is required for virulence in the septicemic plague model in strains lacking a functional ZnuABC system.

To demonstrate that HMWP2 contributes to virulence of *znu* mutants due to Zn^{2+} and not Fe^{3+} uptake, we tested the Δ*psn*::*kan* Δ*znuBC* strain in the septicemic plague model. The Psn receptor, that is required for Fe^{3+} uptake via the Ybt siderophore, is critical for lethal infection during bubonic and pneumonic plague (Fetherston *et al.*, 2010). Unlike HMWP2, Psn is not involved in Zn^{2+} uptake *in vitro*. Thus, we reasoned that a Δ*psn*::*kan* Δ*znuBC* mutant would not show a drastic virulence defect in the septicemic plague model. Indeed, this double mutant remained highly virulent indicating that Fe^{3+} uptake via the Ybt siderophore is not needed for virulence of the Δ*znuBC* mutant during septicemic plague and that the Psn receptor is not involved in Zn^{2+} acquisition *in vivo*. Thus the combination of data from *in vitro* growth and animal experiments strongly suggest that the virulence defect observed for the *irp2 znu* mutants in mice is not due to defects in the acquisition of both Zn^{2+} and Fe^{3+} but rather attributable to the roles of the ZnuABC system and Ybt in Zn^{2+} uptake.

The IM protein YbtX, but not YbtQ, is required for Zn^{2+} acquisition via the Ybt system *in vitro*

Two genes, *ybtP* and *ybtQ*, encoded within a putative *ybtPQXS* operon, are required for Ybt-dependent Fe^{3+} transport into the cell. YbtP and YbtQ are putative IM proteins with both permease and ATPase domains (Fetherston *et al.*, 1999). We tested if these components are also involved in Zn^{2+} transport using a Δ*ybtQX* Δ*znuBC* double mutant. Previous studies have shown that *ybtX* is not required for Fe^{3+} uptake via Ybt (Fetherston *et al.*, 1999). In cPMH2 supplemented with 1.0 μM $FeCl_3$ and 0.6 μM $ZnCl_2$, the growth of this double

mutant was defective compared to that of the Δ*znuBC* and Δ*ybtQX* single mutants. A higher level of $ZnCl_2$ supplementation was required to significantly enhance the growth of the Δ*ybtQX* Δ*znuBC* mutant compared to the Δ*znuBC* mutant (Fig. 7). Addition of $FeCl_3$ to 10 μM did not stimulate growth of the double mutant (data not shown). This demonstrates that the growth defect was due to a defect in Zn^{2+} uptake.

This growth defect was alleviated by complementation with the *ybtPQX* locus expressed from its native promoter on a recombinant plasmid (Fig. 8A). However, a plasmid expressing *ybtPQ* did not complement the growth defect of the Δ*ybtQX* Δ*znuBC* mutant (Fig. 8A) while expression of only *ybtX* did restore the growth of this mutant (Fig. 8B). Based on bioinformatics, YbtX is an IM protein that belongs to the Major Facilitator Superfamily (MFS). Several members of MFS have been shown to be involved in siderophore utilization (Chatfield *et al.*, 2012; Ó Cuív *et al.*, 2004). Our data suggest that YbtX, but not YbtQ, is involved in Zn^{2+} uptake. To further confirm this we constructed and tested an in frame Δ*ybtX* Δ*znuA* mutant. This mutant showed a growth defect similar to that of the double Δ*ybtQX* Δ*znuBC* mutant (data not shown) indicating that YbtX is required for Ybt-dependent Zn^{2+} utilization.

We also used feeding assays with culture supernatants from a Ybt-producing strain and an *irp2::kan* mutant to determine whether secreted siderophore/zincophore supported the growth of strains lacking the Fe^{3+}-Ybt receptor Psn but not the IM protein YbtX (Fig. 9A). Indeed, the growth of a triple Δ*psn irp2::kan* Δ*znuBC* mutant was supported by Ybt-containing supernatant from KIM6+ but not by the Ybt-negative supernatant from the *irp2::kan* mutant KIM6-2046.1. Supernatant from a *ybtU* mutant, KIM6-2071, also failed to stimulate the growth of the Δ*psn irp2::kan* Δ*znuBC* mutant (data not shown). YbtU reduces the middle thiazoline ring to thiazolidine (Fig. 1) and thus it is required for Ybt synthesis (Miller *et al.*, 2002). Finally, we tested purified apo-Ybt for its ability to stimulate the growth of Δ*psn irp2::kan* Δ*znuBC* mutant cells in cPMH2 supplemented with 1.0 μM $FeCl_3$ and 0.6 μM $ZnCl_2$. As expected, addition of apo-Ybt stimulated growth of this mutant similar to the addition of culture supernatants containing Ybt (Fig. 9B). This provides evidence that Ybt in the external environment likely serves as a zincophore. Moreover, Ybt-dependent Zn^{2+} translocation across the OM is independent of TonB and the OM receptor Psn.

In contrast, the Ybt-containing supernatant did not alleviate the growth defect of a quadruple Δ*psn irp2::kan* Δ*ybtX* Δ*znuBC* mutant (Fig. 9A). Thus the IM protein YbtX is essential for Ybt -dependent Zn^{2+} uptake demonstrating that Zn^{2+} uptake via this route uses a pathway completely different from that for Fe^{3+}-Ybt utilization.

Discussion

Zinc is essential for bacterial growth and the development of disease in mammals where it is chelated as a component of nutritional immunity. While some pathogens appear to depend upon the high-affinity Zn^{2+} ABC transporter ZnuABC and its homologues, the mechanisms used to circumvent Zn^{2+} sequestration remain largely unknown. It has been suggested that pathogens may use zincophores analogous to siderophores to scavenge Zn^{2+} from

mammalian hosts (Cerasi *et al.*, 2013; Hood and Skaar, 2012). Previously, we found that a *Y. pestis* Δ*znuBC* mutant retained nearly full virulence in mouse models of bubonic and pneumonic plague (Desrosiers *et al.*, 2010). Our data here provides evidence that *Y. pestis* likely uses the siderophore Ybt as a zincophore to acquire Zn^{2+}.

Several lines of evidence indicate Ybt-dependent Zn^{2+} acquisition by *Y. pestis* under low Zn^{2+} conditions *in vitro.* First, in combination with the Δ*znuBC* mutation, two different *irp2* mutations caused a more severe growth defect compared to the *znu* mutant in cPMH2 medium supplemented with 0.6 μM $ZnCl_2$ and 1.0 μM $FeCl_3$ (Fig. 3). Second, this growth defect was complemented *in trans* by the cloned *irp2* gene or by zinc supplementation to 2.5 μM (Fig. 3 and 4C). Third, analysis of the expression of β-galactosidase from a *znuA′::lacZ* reporter indicates that the *Y. pestis irp2′::kan* mutant was more Zn^{2+}-deficient than its Ybt^{+} parent (Fig. 4A) and the *irp2′::kan* Δ*znuBC* double mutant failed to accumulate significant intracellular Zn^{2+} in cPMH2 medium supplemented to 10 μM $ZnCl_2$ (Fig. 4B). Finally, purified apo-Ybt or culture supernatants containing Ybt but not Ybt-negative culture supernatants supported the growth of a triple Δ*psn irp2′::kan* Δ*znuBC* mutant under low Zn^{2+} conditions (Fig. 9).

Recently, Chaturvedi et al have shown that Ybt binds copper and reduces copper toxicity in an *E. coli* strain producing Ybt and enterobactin (Chaturvedi *et al.*, 2012). In addition, a Ybt-like compound, micacocidin, produced by some Pseudomonads and *Ralstonia solanacearum* chelates Zn^{2+} (micacocidin A), Cu^{2+} (micacocidin B), and Fe^{3+} (micacocidin C) and has anti-mycoplasma activity. A pentyl chain on the salicylate moiety of Ybt is the only structural difference between micacocidin and Ybt (Fig. 1A) (Kobayashi *et al.*, 1998a; Kobayashi *et al.*, 2000; Kobayashi *et al.*, 1998b; Kreutzer *et al.*, 2011). Moreover, two primary siderophores of Pseudomonads, Pyoverdine I (PVDI) and Pyochelin (Pch) have been shown to bind a wide range of divalent cations including Zn^{2+}. These non-iron PVDI and Pch complexes appear to function in cation homeostasis and reduction of metal toxicities. These studies demonstrate effective chelation of non-iron metals by these two siderophores; however, acquisition of these metals, particularly Zn^{2+} and Mn^{2+}, for nutritional use has not been assessed. Note that Pch (Fig. 1B) has a structure nearly identical to Ybt minus the malonyl linker group and the second thiazoline ring (Brandel *et al.*, 2012; Braud *et al.*, 2009a; Braud *et al.*, 2009b; Braud *et al.*, 2010; Schalk and Guillon, 2013; Schalk *et al.*, 2011). In *S. coelicolor*, coelibactin, a non-ribosomally synthesized molecule whose expression is regulated by Zur has been proposed as a zincophore. However, Zn^{2+} chelation and acquisition by coelibactin has not been demonstrated. Coelibactin has a predicted structure with similarities to Ybt and micacocidin, at least prior to further putative enzymatic tailoring (Hesketh *et al.*, 2009; Zhao *et al.*, 2012). The secreted protein, Pra1, has a proven role in Zn^{2+} scavenging in *C. albicans* (Citiulo *et al.*, 2012) but this system is more analogous to the bacterial hemophore system (Cescau *et al.*, 2007) – both are ribosomally synthesized small proteins.

Pyridine-2,6-bis(thiocarboxylic acid) (PDTC), a small siderophore (198 daltons) produced by some Pseudomonads forms 1:1 or 1:2 complexes with a number of biometals with the highest affinity for Fe^{3+}. Growth of *P. putida* is stimulated by supplementation with micromolar Zn^{2+} only if the strain produces PDTC. However, Zn^{2+} acquisition by PDTC

appears to be much less efficient than Fe^{3+} acquisition (Cortese *et al.*, 2002; Leach *et al.*, 2007). *P. putida* PDTC and *Y. pestis* Ybt are the only two examples of siderophores/zincophores with proven roles in Zn^{2+} acquisition. Whether siderophore/zincophore-dependent Zn^{2+} uptake is wide-spread in bacteria remains to be determined.

Although the *Y. pestis* OM receptor Psn and the TonB system are required for Fe^{3+} uptake via the Ybt siderophore, neither of these are needed for Ybt-dependent Zn^{2+} acquisition (Fig. 6). In Gram-negative bacteria, involvement of the TonB-ExbBD complex in siderophore-Fe^{3+} uptake via an OM receptor is a paradigm for iron acquisition via siderophores (Miethke and Marahiel, 2007). TonB-dependent receptors also appear to be needed for uptake of Zn^{2+}-siderophore complexes in *Pseudomonas* species. In *P. putida*, the TonB-dependent OM receptor PdtK is required for efficient growth stimulation by Zn^{2+}-PDTC complexes (Leach *et al.*, 2007). Hannauer *et al*. observed accumulation of Zn^{2+}-PVD complexes into the periplasm of *Peusdomonas aeruginosa* cells only when the TonB-dependent OM FpvA receptor was present. In this instance unwanted metals were then effluxed from the periplasm (Hannauer *et al.*, 2012). However, there are several examples of siderophore uptake by TonB-independent receptors. *Legionella pneumophila* and *Fransicella tularensis* each lack the TonB-ExbBD system. However, the OM receptor proteins LbtU and FslE are involved in Fe^{3+}-siderophore utilization by these two pathogens (Chatfield *et al.*, 2011; Ramakrishnan *et al.*, 2008; Ramakrishnan *et al.*, 2012). Use of ferrioxamines B and E are dependent upon TonB and the TonB-dependent OM receptor FoxA in *Salmonella enterica*; however a *tonB* mutant still exhibited reduced utilization of these two siderophores (Kingsley *et al.*, 1999). How these ferrisiderophores or Zn^{2+}-siderophore/zincophore complexes are transported through the OM remains unanswered. In *Y. pestis*, a putative OM receptor for Ybt-dependent Zn^{2+} utilization could rely upon the TolABQR system (Lloubès *et al.*, 2012) for providing energy. While this is a possibility, the mechanism for translocation across the OM remains to be elucidated.

Transport of ferrisiderophores through the cytoplasmic membrane of bacteria typically requires ABC permeases (Miethke and Marahiel, 2007). In *Y. pestis*, the putative IM ABC transporter YbtPQ is essential for Fe^{3+}-Ybt utilization (Fetherston *et al.*, 1999). Unlike Fe^{3+}-Ybt uptake, this study indicates that a predicted MFS member, YbtX (with no known role in Fe^{3+} uptake), not YbtPQ, is critical for Ybt-dependent Zn^{2+} import (Fig. 7 and 8). Strikingly, another MFS member, PdtE, was required for utilization of Zn^{2+}-PDTC complexes in *P. putida* (Leach *et al.*, 2007). MFS type proteins have been shown to be involved in both siderophore uptake and efflux (Chatfield *et al.*, 2012). Several MFS members including RhtX, FptX (orthologs of YbtX) and LbtC are needed for Fe^{3+} uptake via the rhizobactin, pyochelin and legiobactin siderophores in *Sinorhizobium meliloti, P. aeruginosa* and *L. pneumophila*, respectively (Chatfield *et al.*, 2012; Michel *et al.*, 2007; Ó Cuív *et al.*, 2004). However, in our experiments, inactivation of *ybtX* did not prevent secretion of the Ybt siderophore or cause any growth defects in metal-chelated medium, traits generally found in bacteria with mutations in genes encoding siderophore efflux pumps (Crouch *et al.*, 2008; Fetherston *et al.*, 1999; Furrer *et al.*, 2002) suggesting that YbtX is not required for Ybt export. Thus, Ybt-dependent uptake of Fe^{3+} and Zn^{2+} appear to require completely different transport routes through the OM and IM (Fig. 10). This

suggests that Ybt complexes with Fe^{3+} and Zn^{2+} may have sufficiently different structural conformations to require separate transport systems. Two isomers of the Pch siderophore, which has a similar structure to Ybt, use different OM receptors and IM transporters. In *P. aeruginosa*, Fe^{3+}-Pch translocates through the OM and IM using the OM receptor FptA and MFS permease FptX, respectively, while transport of its isoform ferri-enantio-Pch occurs via the OM receptor FetA and IM ABC transporter FetDE in *P. fluorescens*. These transport components are not interchangeable – FptA and FptX transports Fe^{3+}-Pch not ferri-enantio-Pch (Youard *et al.*, 2011).

Here, we propose a model for Zn^{2+} acquisition in *Y. pestis* by the ZnuABC and Ybt siderophore/zincophore systems using two independent uptake routes (Fig. 10). Under *in vitro* conditions, Zn^{2+} may enter the cell passively through OM porins. In the periplasm, ZnuA chaperones Zn^{2+} to the ZnuBC ABC transporter required for the active transport of Zn^{2+} across the IM. Although ZnuABC is a major Zn^{2+} uptake system under the *in vitro* growth conditions we have used (Fig. 3A; (Desrosiers *et al.*, 2010), both Zn^{2+} transport systems appear to be equally important *in vivo*. Strains with a mutation in either system retain nearly full virulence in the septicemic plague model while a double mutant is highly attenuated. We propose that Ybt is secreted to the external environment where it chelates Zn^{2+} and serves as a zincophore to bring this essential metal into the bacterial cell using a TonB-independent receptor or porin. How Zn^{2+} translocates through the OM remains to be determined but it is likely to be an energy dependent process. Subsequent transport of Zn^{2+} or Zn^{2+}-Ybt from the periplasm into the cytoplasm requires YbtX in the IM. Finally, the mechanism for removing Zn^{2+} from Ybt is uncharacterized.(Fig. 10).

Under *in vitro* conditions when low concentrations of unchelated Zn^{2+} are present, the growth of many bacterial species is dependent on ZnuABC or a related C9 family ABC Zn^{2+} transporter. *In vivo*, mutations in genes encoding the Znu family of transporters cause a severe loss of virulence or colonization by *B. abortus, C. jejuni, M. cararrhalis, P. multocida, N. gonorrhoeae, S.* Typhimurium, *S. penumoniae, S. pyogenes,* and *Y. ruckeri* (Ammendola *et al.*, 2007; Bayle *et al.*, 2011; Campoy *et al.*, 2002; Dahiya and Stevenson, 2010; Davis *et al.*, 2009; Garrido *et al.*, 2003; Kim *et al.*, 2004; Lim *et al.*, 2008; Liu *et al.*, 2012; Murphy *et al.*, 2013; Plumptre *et al.*, 2014; Weston *et al.*, 2009; Yang *et al.*, 2006). Clearly, in the mammalian host, the *Y. pestis* ZnuABC transporter acquires sufficient Zn^{2+} to cause disease despite chelation by host proteins. In the inflamed gut, the Znu system of *Salmonella* overcomes Zn^{2+}-chelation by calprotectin (Liu *et al.*, 2012). How Zn^{2+} is removed from calprotectin and/or other host Zn^{2+}-sequestering proteins is unknown. The *N. meningitidis* TonB-dependent OM receptor protein CbpA has been recently reported to bind calprotectin, allowing its utilization as a Zn^{2+} source (Stork *et al.*, 2013). Another, possibility is that inflammation and necrosis may release Zn^{2+} from some host proteins.

In other bacterial pathogens, *A. baumanii*, uropathogenic *E. coli, H. ducreyi, H. influenzae, L. monocytogenes, P. mirabilis, Vibrio parahaemoliticus,* and *Y. pestis,* mutations in *znu* do not affect virulence or have a subtle effect on virulence or colonization (Desrosiers *et al.*, 2010; Hood *et al.*, 2012; Lewis *et al.*, 1999; Liu *et al.*, 2013; Nielubowicz *et al.*, 2010; Rosadini *et al.*, 2011; Sabri *et al.*, 2009) suggesting that additional Zn^{2+} uptake systems are involved in the virulence of these bacteria. Indeed, in uropathogenic *E. coli, H. influenzae,*

L. monocytogenes, and *S.* Typhimurium, mutation of a second Zn^{2+} transporter in a *znu* background further decreased virulence or colonization. Thus, in these pathogens, both ZnuABC and the 2nd Zn^{2+} transporter contribute to virulence (Cerasi *et al.*, 2014; Corbett *et al.*, 2012; Rosadini *et al.*, 2011; Sabri *et al.*, 2009).

A *Y. pestis irp2* mutant is avirulent in the mouse model of bubonic plague and highly attenuated in the pneumonic plague model (Fetherston *et al.*, 2010). Consequently, in this study, we have used a mouse model of septicemic plague in which a Δ*pgm* mutant (which lacks the entire Ybt system) is known to be highly virulent (Bearden and Perry, 1999; Jackson and Burrows, 1956; Une and Brubaker, 1984). Here we show an absolute requirement for Zn^{2+} acquisition for *Y. pestis* virulence in septicemic plague. The double *irp2 znu* mutants had a $>10^5$-fold attenuation compared to the Ybt^+ Znu^+ parent strain (Table 1). Since a *Y. pestis znu* mutant is highly virulent in all three mouse plague models (Desrosiers *et al.*, 2010) (Table 1), these data suggest that Ybt-dependent Zn^{2+} uptake compensates for the loss of Zn^{2+} acquisition in mice by a *znu* mutation in *Y. pestis*. Since the *irp2* single mutant is highly virulent in the septicemic plague model, it appears that the ZnuABC and Ybt serve redundant functions for Zn^{2+} acquisition in mammals with either being sufficient to cause disease. It is also possible that Ybt may remove Zn^{2+} from mammalian proteins. *Y. pestis* is the first pathogen with interrelated siderophore/zincophore systems involved in Zn^{2+} and Fe^{3+} acquisition *in vitro* and *in vivo*.

Experimental Procedures

Bacterial strains, plasmids, primers and growth conditions

The bacterial strains, plasmids and primers used in this study are listed in Table S1 in supporting information. All bacterial strains are stored in glycerol stocks (Beesley *et al.*, 1967) at -80°C. *E. coli* strains DH5α and DH5α (λ*pir*) were used in the construction and maintenance of recombinant plasmids and were grown in Luria broth (LB) or on LB agar at 28-37°C. Select agent-exempt *Y. pestis* strains lacking the pCD1 virulence plasmid or the 102-kb chromosomal *pgm* locus were used for the construction of all mutants and *in vitro* studies. *Y. pestis* strain designations that lack a plus sign have a *pgm* deletion or a mutation within the *pgm* locus, which encodes the ∼29 kb *ybt* locus/high pathogenicity island. The *pgm* locus can be lost spontaneously *in vitro* at a rate of 10^{-5} (Brubaker, 1969; Fetherston and Perry, 1994; Perry and Fetherston, 2011). From glycerol stocks, *Y. pestis* strains were inoculated onto Tryptose Blood Agar Base (TBA) (Difco) or a modified Congo Red (CR) agar (Surgalla and Beesley, 1969) consisting of TBA supplemented with 0.2% (w/v) galactose, 1% (w/v) CR and $ZnSO_4$ or $ZnCl_2$ to a final concentration of 100 μM and grown at 32-33°C for 2 days. Formation of red colonies on CR plates indicates that the strain has retained the *pgm* locus and a red colony was inoculated onto TBA slants. From slants, *Y. pestis* strains were grown in Heart Infusion Broth (HIB) with indicated supplementations or cPMH2 at 30-37°C. Where necessary, ampicillin (Ap), kanamycin (Km), spectinomycin (Spc) or streptomycin (Sm) were used at final concentrations of 100, 50, 25 and 50 μg ml^{-1}, respectively. TBA medium supplemented with 5% sucrose was used to cure suicide vectors as previously described (Fetherston *et al.*, 1999).

Comparison of bacterial growth under metal-deficient conditions

All glassware used for Zn- and/or Fe-restricted growth studies was soaked overnight in a saturated chromic acid solution to remove contaminating metals and copiously rinsed in deionized water. For growth studies, *Y. pestis* strains were inoculated from TBA slants to an OD_{620} of ~ 0.1 in the chemically defined medium, cPMH2, which had been extracted prior to use with Chelex-100 resin (Bio-Rad Laboratories), with or without $ZnCl_2$ or $FeCl_3$ supplementation to various concentrations. Unsupplemented cPMH2 medium has a residual Zn^{2+} concentration of ~0.5 μM (Desrosiers *et al.*, 2010; Gong *et al.*, 2001). Cultures were aerated (250 rpm) at 37°C with culture volumes ~10-20% of the volumes of treated glassware or plastic conical tubes (Falcon). Growth through one or two transfers (~3-4 or 6-8 generations) was used to acclimate cells to cPMH2 and varying Zn^{+2} or Fe^{+3} conditions prior to use in all experimental studies, unless otherwise indicated. Growth of the cultures was monitored by determining the OD_{620} with a Genesys5 spectrophotometer (Spectronic Instruments, Inc.).

Mutant strain constructions

Suicide plasmids pSucZnu3.5, pKNGΔznuA, pKNGΔtonB2, pPSN15, pCIRP498.8 and pCVDybtX (Table S1 in supporting information) were used to introduce mutations in *znuBC*, *znuA*, *hasB*, *psn*, *irp2*, and *ybtX*, respectively, into various *Y. pestis* KIM strains by allelic exchange as described previously (Fetherston *et al.*, 1995). The λ red recombinase method (Datsenko and Wanner, 2000; Lathem *et al.*, 2007) was used to inactivate *y1329-y1330* and *y1245*. The PCR product for replacement of *y1329-1330* in KIM6-2077+ with a *kan* cassette was prepared using y1329red-Forw and y1330red-Rev primers and pKD4 as a template. In a double *znu y1329-1330* mutant carrying pWL204, *y1245* was replaced with a *cat* cassette from pKD3 using y1245-KMI and y1245-KMII primers. All genetic mutations were confirmed by PCR using primers listed in Table S1 in supporting information.

To construct the suicide vector pKNGΔznuA with an in-frame *znuA* deletion, pZnu2 (Desrosiers *et al.*, 2010) was digested with *Hind*III and *Pst*I to release a 1.9 kb fragment that was cloned into the same sites in pBluescript-KS to yield pBSZnuA. A 156 amino acid deletion within ZnuA (Fig. S2) was created by ligating a *Hind*III/*Xmn*I fragment and a *Pst*I/*Fsp*I fragment from pBSZnuA into the *Hind*III and *Pst*I sites of pBluescript-KS. This plasmid, called pBSΔznuA was cut with *Sal*I and *Xba*I and the 1.5 kb piece containing the deleted version of *znuA* was ligated into the same sites of pKNG101, resulting in pKNGΔZnuA.

Complementation of the *znuBC* mutation

An ~3 kb *Stu*I/*Age*I fragment that contains the coding sequences for ZnuA, B and C, was isolated from pZnu2 and cloned into the *Stu*I and *Xma*I sites of pUC18R6K-mini-Tn7T-Km to generate the Znu integration vector, pUCR6K-ZnuABC-Km. The plasmid was electroporated, along with the Tn*7* transposase expression vector, pTNS2, into KIM6-2077+ and KIM6-2077. Kanamycin resistant strains containing the mini-Tn*7* transposon with *znuABC*$^+$ integrated at the *att*Tn*7* site were confirmed by hybridization and PCR. A 240 bp DNA fragment encompassing parts of *znuA* and *znuC* ORFs as well as the intergenic region between the *znuA* and *znuCB* operons was DIG-labeled by PCR with primers ZnuC.3 and

ZnuC.5 and used as a probe against *Eco*RI and *Hind*III/*BamH*I digested genomic DNA from tested strains. For verification of *znuABC*$^{+}$ integration into the chromosomal *att*Tn*7* site by PCR, ZnuA 5.3 and attTn7Yp-Fwd primers were used. The resulting strains named KIM6-2077.10+ and KIM6-2077.10.

Construction of a YbtX expressing plasmid

To delete the *ybtPQ* genes (~ 3.4 kb) from pYbtPQX, primers ybtPQdel_F and ybtPQdel_R were used in reverse splicing by overlap extension PCR. Following the reaction, *Dpn*I was added to digest template DNA; the PCR product was precipitated with ethanol and transformed into *E. coli* DH5α chemically competent cells. Clones with the appropriate *ybtPQ* deletion were detected by PCR and confirmed by sequencing (ACGT Inc.). The resulting plasmid, pYbtX, was introduced into KIM6-2077.13 for complementation studies.

β-Galactosidase assays

The β-galactosidase activities from *znuA*::*lacZ* or *irp2*::*lacZ* reporter fusions were measured in *Y. pestis* strains carrying the reporter plasmids pEUZnu1 or pEUIrp2, respectively (Desrosiers *et al.*, 2010; Perry *et al.*, 2003a). To compare *znuA*::*lacZ* reporter activity in Δ*znuBC* (KIM6-2077+) and *irp2*::*kan* Δ*znuBC* (KIM6-2077.7) mutants, the strains were grown at 33-34°C overnight on TBA slants supplemented with Spc and $ZnCl_2$ at a final concentrations of 25 μg ml^{-1} and 10 μM, respectively. The cells were resuspended in cPMH2 supplemented with Spc and various concentrations of $ZnCl_2$ and/or $FeCl_3$ to an OD_{620} ~ 0.1, grown at 37°C for ~ 3 generations and harvested. To compare *znuA*::*lacZ* reporter activities in the KIM6+ parent to *irp2*::*kan* (KIM6-2046.1) and Δ*znuBC* mutants, the strains were grown on TBA slants with Spc at 33-34°C overnight. The cells were grown through two transfers in cPMH2 with Spc for 5.5-6.5 generations before harvesting. To monitor *irp2*::*lacZ* reporter activities in the KIM6+ and Δ*znuBC* mutant, TBA/Spc pre-grown cells were propagated through two transfers in cPMH2/Spc with or without $ZnCl_2$ or $FeCl_3$ for 4.5-5.5 generations before collecting samples. β-Galactosidase activities from whole-cell lysates were measured by monitoring the hydrolysis of *o*-nitrophenyl-β-D-galactopyranoside spectrophotometrically with the results expressed in Miller units (Miller, 1992).

Purification of apo-Ybt

Apo-Ybt was purified in a multi-step procedure modified from previous methods (Miller and DeMoll, 2011; Miller *et al.*, 2010). No iron was added to the spent media before extraction. Eight liters of spent media were extracted in 500 ml aliquots with three washes of 200 ml ethyl acetate. The organic layers were collected, combined, and the solvent was removed by rotary evaporation at 40°C. The material was then re-dissolved in ~5 ml of 100% ethanol. The crude material was then diluted to 50 ml with 18 MΩ water for the next step of purification.

Final Ybt purification was performed on a Combiflash Rf. Crude Ybt was dissolved in a 10:1 water-ethanol solution, loaded onto a 2.5 g pre-packed C18 reverse phase cartridge, and purified on a 4.3 g C18 reverse phase column with water and acetonitrile as the mobile phase. The separation was achieved by using the following gradient: 10% acetonitrile for 3

mins followed by a linear gradient from 20% to 60% acetonitrile over 25 minutes (Retention time ≈ 13 min). Fractions were collected every 1 minute. Fractions containing Ybt were concentrated in vacuo and the purification was repeated.

Final fractions were then collected and concentrated to dryness via rotary evaporation at 40°C. The identity and purity of authentic Ybt in each stage of purification was confirmed via mass spectrophotometry using an Agilent 6224 TOF LC/MS equipped with the Agilent 1260 HPLC system and MassHunter software. The instrument was equipped with an Agilent Extend C-18 column (1.8 μm, 2.1 × 50 mm) with mobile phase consisting of mass spectrophotometry grade water (with 0.1% formic acid and 0.1% methanol) and acetonitrile (with 0.1% formic acid) and operated in positive ion mode (3500V Vcap, 750V OctRF Vpp, 65V skimmer, 135V fragmenter, 40 psi Nebulizer gas, 12 liter/min drying gas, and 325 C gas temperature). Samples were eluted from with a linear gradient of 5 to 100% acetonitrile at 0.3 ml/min over 15 minutes. Authentic Ybt eluted at approximately 7.66 minutes with an M+1 mass of 482.1250 and an M+2 mass 241.5643 of in agreement with the predicted M+1 and M+2 masses of 482.1236 and 241.5655 respectively.

Feeding assays with culture supernatants and purified apo-Ybt

Ybt-containing and Ybt-negative culture supernatants were obtained from KIM6+ and the *irp2::kan* mutant, respectively, grown for two transfers in cPMH2 at 37°C and filter sterilized as previously described (Miller *et al.*, 2010). For Ybt supernatant assays, *Y. pestis* recipient strains, Δ*psn irp2::kan* Δ*znuBC* (KIM6-2077.18) and Δ*psn irp2::kan* Δ*ybtX* Δ*znuBC* (KIM6-2077.19) were grown in cPMH2 supplemented with 0.6 μM $ZnCl_2$ and 1μM $FeCl_3$ at 37°C for about 4-5 generations before they were back diluted to an OD_{620} of ∼ 0.1 in the same medium containing 50% (v/v) of culture supernatants from either KIM6+, the *irp2::kan* or *ybtU* mutants. For apo-Ybt utilization assays, the Δ*psn irp2::kan* Δ*znuBC* recipient strain was grown overnight as above and back diluted to an OD_{620} of ∼ 0.1 in the same medium with the addition of purified apo-Ybt in ethanol (0.25 or 1 μl of a 10 mM concentration in ethanol per 1.5 ml) or ethanol alone (1 μl per 1.5 ml). Bacteria were cultivated at 37°C overnight and final OD_{620}s were measured.

Virulence testing

Construction and testing of potentially virulent strains was performed in a CDC-approved BSL3 laboratory following Select Agent regulations using procedures approved by the University of Kentucky Institutional Biosafety Committee. All animal care and experimental procedures were conducted in accordance with the *Animal Welfare Act, Guide for the Care and Use of Laboratory Animals, PHS Policy and the U.S. Government Principals for the Utilization of and Care for Vertebrate Animals in Teaching, Research, and Training* and approved by the University of Kentucky Institutional Animal Care and Use Committee. The University of Kentucky Animal Care Program is accredited by the Association for the Assessment and Accreditation of Laboratory Animal Care, Inc.

Y. pestis strains were transformed with pCD1Ap by electroporation (Fetherston *et al.*, 1995), plasmid profiles analyzed, and transformant phenotypes determined on CR agar (Surgalla and Beesley, 1969) and magnesium-oxalate plates (Higuchi and Smith, 1961). After growth

at 37°C in cPMH2 with or without 2.5 mM $CaCl_2$, culture supernatants were tested for LcrV secretion by Western blot using polyclonal antisera against LcrV (provided by R.R. Brubaker).

For mouse infections, several colonies of *Y. pestis* from an agar plate were streaked onto a TBA slant and grown overnight at 30°C. Cells were washed off the slant and inoculated to an OD_{620} of ~0.1 in HIB supplemented with 50 μg Ap/ml, 0.2% xylose, 2.5 mM $CaCl_2$ and 10μM $ZnCl_2$ and grown at 37°C overnight. These cultures were diluted to an OD_{620} of ~0.1 into the same medium but without zinc supplementation and grown at 37°C for ~2 generations. The cultures were centrifuged and cell pellets were resuspended in mouse isotonic phosphate-buffered saline (PBS; 149 mM NaCl, 16 mM Na_2HPO_4, 4 mM NaH_2PO_4 [pH 7.0]). 0.1 ml of 10-fold serially diluted bacterial suspensions was injected retro-orbitally (via the retro-orbital plexus) into groups of four 6- to 8-week old female Swiss Webster mice (Hsd: :ND4) sedated by inhalation of isoflurane-oxygen or by intraperitoneally injecting a mixture of 100 μg of ketamine and 10 μg of xylazine per kg of body weight. Appropriate serial dilutions of the cultures used for injections were inoculated onto TBA plates containing Ap (30-50 μg ml^{-1}), 2.5 mM $CaCl_2$ and 10 or 100 μM $ZnCl_2$ and colonies were counted after 2-3 days of incubation at 30-33°C. Mice were observed daily for 2 weeks and LD_{50} values were calculated according to the method of Reed and Muench (Reed and Muench, 1938).

Supplementary Material

Refer to Web version on PubMed Central for supplementary material.

Acknowledgments

This work was supported by Public Health Services grant AI33481 from the U.S. National Institutes of Health. We thank Will Arnold for help with the construction of some mutants and some preliminary experiments and Bob Brubaker for providing antisera against LcrV.

References

Althaus EW, Outten CE, Olson KE, Cao H, O'Halloran TV. The ferric uptake regulation (Fur) repressor is a zinc metalloprotein. Biochemistry. 1999; 38:6559–6569. [PubMed: 10350474]

Ammendola S, Pasquali P, Pistoia C, Petrucci P, Petrarca P, Rotilio G, Battistoni A. High-affinity Zn^{2+} uptake system ZnuABC is required for bacterial zinc homeostasis in intracellular environments and contributes to the virulence of *Salmonella enterica*. Infect Immun. 2007; 75:5867–5876. [PubMed: 17923515]

Andreini C, Banci L, Bertini I, Rosato A. Zinc through the three domains of life. J Proteome Res. 2006; 5:3173–3178. [PubMed: 17081069]

Bayle L, Chimalapati S, Schoehn G, Brown J, Vernet T, Durmort C. Zinc uptake by *Streptococcus pneumoniae* depends on both AdcA and AdcAII and is essential for normal bacterial morphology and virulence. Mol Microbiol. 2011; 82:904–916. [PubMed: 22023106]

Bearden SW, Fetherston JD, Perry RD. Genetic organization of the yersiniabactin biosynthetic region and construction of avirulent mutants in *Yersinia pestis*. Infect Immun. 1997; 65:1659–1668. [PubMed: 9125544]

Bearden SW, Perry RD. The Yfe system of *Yersinia pestis* transports iron and manganese and is required for full virulence of plague. Mol Microbiol. 1999; 32:403–414. [PubMed: 10231495]

Beesley ED, Brubaker RR, Janssen WA, Surgalla MJ. Pesticins. III. Expression of coagulase and mechanism of fibrinolysis. J Bacteriol. 1967; 94:19–26. [PubMed: 6027989]

Brandel J, Humbert N, Elhabiri M, Schalk IJ, Mislin GLA, Albrecht-Gary AM. Pyochelin, a siderophore of Pseudomonas aeruginosa: physicochemical characterization of the iron(iii), copper(ii) and zinc(ii) complexes. Dalton Trans. 2012; 41:2820–2834. [PubMed: 22261733]

Braud A, Geoffroy V, Hoegy F, Mislin GLA, Schalk IJ. Presence of the siderophores pyoverdine and pyochelin in the extracellular medium reduces toxic metal accumulation in *Pseudomonas aeruginosa* and increases bacterial metal tolerance. Environ Microbiol Rep. 2010; 2:419–425. [PubMed: 23766115]

Braud A, Hannauer M, Mislin GLA, Schalk IJ. The *Pseudomonas aeruginosa* pyochelin-iron uptake pathway and its metal specificity. J Bacteriol. 2009a; 191:3517–3525. [PubMed: 19329644]

Braud A, Hoegy F, Jezequel K, Lebeau T, Schalk IJ. New insights into the metal specificity of the *Pseudomonas aeruginosa* pyoverdine - iron uptake pathway. Environ Microbiol. 2009b; 11:1079–1091. [PubMed: 19207567]

Brubaker RR. Mutation rate to nonpigmentation in *Pasteurella pestis*. J Bacteriol. 1969; 98:1404–1406. [PubMed: 5788712]

Campoy S, Jara M, Busquets N, Pérez de Rozas AM, Badiola I, Barbé J. Role of the high-affinity zinc uptake *znuABC* system in *Salmonella enterica* serovar typhimurium virulence. Infect Immun. 2002; 70:4721–4725. [PubMed: 12117991]

Cerasi M, Ammendola S, Battistoni A. Competition for zinc binding in the host-pathogen interaction. Front Cell Infect Microbiol. 2013; 3:108. [PubMed: 24400228]

Cerasi M, Liu JZ, Ammendola S, Poe AJ, Petrarca P, Pesciaroli M, et al. The ZupT transporter plays an important role in zinc homeostasis and contributes to *Salmonella enteric*a virulence. Metallomics. 2014; 6:845–853. [PubMed: 24430377]

Cescau S, Cwerman H, Létoffé S, Delepelaire P, Wandersman C, Biville F. Heme acquisition by hemophores. BioMetals. 2007; 20:603–613. [PubMed: 17268821]

Chatfield CH, Mulhern BJ, Burnside DM, Cianciotto NP. *Legionella pneumophila* LbtU acts as a novel, TonB-independent receptor for the legiobactin siderophore. J Bacteriol. 2011; 193:1563–1575. [PubMed: 21278293]

Chatfield CH, Mulhern BJ, Viswanathan VK, Cianciotto NP. The major facilitator superfamily-type protein LbtC promotes the utilization of the legiobactin siderophore by *Legionella pneumophila*. Microbiology. 2012; 158:721–735. [PubMed: 22160401]

Chaturvedi KS, Hung CS, Crowley JR, Stapleton AE, Henderson JP. The siderophore yersiniabactin binds copper to protect pathogens during infection. Nat Chem Biol. 2012; 8:731–736. [PubMed: 22772152]

Citiulo F, Jacobsen ID, Miramón P, Schild L, Brunke S, Zipfel P, et al. *Candida albicans* scavenges host zinc via Pra1 during endothelial invasion. PLoS Pathog. 2012; 8:e1002777. [PubMed: 22761575]

Corbett D, Wang J, Schuler S, Lopez-Castejon G, Glenn S, Brough D, et al. Two zinc uptake systems contribute to the full virulence of *Listeria monocytogenes* during growth i*n vitro* and i*n vivo*. Infect Immun. 2012; 80:14–21. [PubMed: 22025520]

Corbin BD, Seeley EH, Raab A, Feldmann J, Miller MR, Torres VJ, et al. Metal chelation and inhibition of bacterial growth in tissue abscesses. Science. 2008; 319:962–965. [PubMed: 18276893]

Cortese MS, Paszczynski A, Lewis TA, Sebat JL, Borek V, Crawford RL. Metal chelating properties of pyridine-2,6-bis(thiocarboxylic acid) produced by Pseudomonas spp. and the biological activities of the formed complexes. BioMetals. 2002; 15:103–120. [PubMed: 12046919]

Crouch MLV, Castor M, Karlinsey JE, Kalhorn T, Fang FC. Biosynthesis and IroC-dependent export of the siderophore salmochelin are essential for virulence of *Salmonella enterica* serovar Typhimurium. Mol Microbiol. 2008; 67:971–983. [PubMed: 18194158]

Dahiya I, Stevenson RMW. The ZnuABC operon is important for *Yersinia ruckeri* infections of rainbow trout, *Oncorhynchus mykiss* (Walbaum). J Fish Dis. 2010; 33:331–340. [PubMed: 20070462]

Datsenko KA, Wanner BL. One-step inactivation of chromosomal genes in *Escherichia coli* K-12 using PCR products. Proc Natl Acad Sci U S A. 2000; 97:6640–6645. [PubMed: 10829079]

Davis LM, Kakuda T, DiRita VJ. A *Campylobacter jejuni znuA* orthologue is essential for growth in low-zinc environments and chick colonization. J Bacteriol. 2009; 191:1631–1640. [PubMed: 19103921]

Desrosiers DC, Bearden SW, Mier I Jr, Abney J, Paulley JT, Fetherston JD, et al. Znu is the predominant zinc importer in *Yersinia pestis* during *in vitro* growth but is not essential for virulence. Infect Immun. 2010; 78:5163–5177. [PubMed: 20855510]

Fetherston JD, Bertolino VJ, Perry RD. YbtP and YbtQ: two ABC transporters required for iron uptake in *Yersinia pestis*. Mol Microbiol. 1999; 32:289–299. [PubMed: 10231486]

Fetherston JD, Kirillina O, Bobrov AG, Paulley JT, Perry RD. The yersiniabactin transport system is critical for the pathogenesis of bubonic and pneumonic plague. Infect Immun. 2010; 78:2045–2052. [PubMed: 20160020]

Fetherston JD, Lillard JW Jr, Perry RD. Analysis of the pesticin receptor from *Yersinia pestis*: role in iron-deficient growth and possible regulation by its siderophore. J Bacteriol. 1995; 177:1824–1833. [PubMed: 7896707]

Fetherston JD, Perry RD. The pigmentation locus of *Yersinia pestis* KIM6+ is flanked by an insertion sequence and includes the structural genes for pesticin sensitivity and HMWP2. Mol Microbiol. 1994; 13:697–708. [PubMed: 7997181]

Foote JW, Delves HT. Albumin bound and a_2 -macroglobulin bound zinc concentrations in the sera of healthy adults. J Clin Pathol. 1984; 37:1050–1054. [PubMed: 6206098]

Forman S, Paulley JT, Fetherston JD, Cheng YQ, Perry RD. *Yersinia* ironomics: comparison of iron transporters among *Yersinia pestis* biotypes and its nearest neighbor, *Yersinia pseudotuberculosis*. BioMetals. 2010; 23:275–294. [PubMed: 20049509]

Furrer JL, Sanders DN, Hook-Barnard IG, McIntosh MA. Export of the siderophore enterobactin in *Escherichia coli*: involvement of a 43 kDa membrane exporter. Mol Microbiol. 2002; 44:1225–1234. [PubMed: 12068807]

Gabbianelli R, Scotti R, Ammendola S, Petrarca P, Nicolini L, Battistoni A. Role of ZnuABC and ZinT in *Escherichia coli* O157:H7 zinc acquisition and interaction with epithelial cells. BMC Microbiol. 2011; 11:36. [PubMed: 21338480]

Garrido ME, Bosch M, Medina R, Llagostera M, Pérez de Rozas AM, Badiola I, Barbé J. The high-affinity zinc-uptake system *znuACB* is under control of the iron-uptake regulator (*fur*) gene in the animal pathogen *Pasteurella multocida*. FEMS Microbiol Lett. 2003; 221:31–37. [PubMed: 12694907]

Gong S, Bearden SW, Geoffroy VA, Fetherston JD, Perry RD. Characterization of the *Yersinia pestis* Yfu ABC iron transport system. Infect Immun. 2001; 67:2829–2837. [PubMed: 11292695]

Graham AI, Hunt S, Stokes SL, Bramall N, Bunch J, Cox AG, et al. Severe zinc depletion of Escherichia coli: Roles for high-affinity zinc binding by ZinT, zinc transport and zinc-independent proteins. J Biol Chem. 2009; 284:18377–18389. [PubMed: 19377097]

Grass G, Wong MD, Rosen BP, Smith RL, Rensing C. ZupT Is a Zn(II) uptake system in *Escherichia coli*. J Bacteriol. 2002; 184:864–866. [PubMed: 11790762]

Hannauer M, Braud A, Hoegy F, Ronot P, Boos A, Schalk IJ. The PvdRT-OpmQ efflux pump controls the metal selectivity of the iron uptake pathway mediated by the siderophore pyoverdine in *Pseudomonas aeruginosa*. Environ Microbiol. 2012; 14:1696–1708. [PubMed: 22187978]

Hantke K. Bacterial zinc uptake and regulators. Curr Opin Microbiol. 2005; 8:196–202. [PubMed: 15802252]

Hesketh A, Kock H, Mootien S, Bibb M. The role of *absC*, a novel regulatory gene for secondary metabolism, in zinc-dependent antibiotic production in *Streptomyces coelicolor* A3(2). Mol Microbiol. 2009; 74:1427–1444. [PubMed: 19906184]

Higuchi K, Smith JL. Studies on the nutrition and physiology of *Pasteurella pestis*. VI. A differential plating medium for the estimation of the mutation rate to avirulence. J Bacteriol. 1961; 81:605–608. [PubMed: 13714203]

Hood MI, Mortensen BL, Moore JL, Zhang Y, Kehl-Fie TE, Sugitani N, et al. Identification of an *Acinetobacter baumannii* zinc acquisition system that facilitates resistance to calprotectin-mediated zinc sequestration. PLoS Pathog. 2012; 8:e1003068. [PubMed: 23236280]

Hood MI, Skaar EP. Nutritional immunity: transition metals at the pathogen-host interface. Nat Rev Microbiol. 2012; 10:525–537. [PubMed: 22796883]

Jackson S, Burrows TW. The virulence-enhancing effect of iron on non-pigmented mutants of virulent strains of *Pasteurella pestis*. Br J Exp Pathol. 1956; 37:577–583. [PubMed: 13396142]

Karlinsey JE, Maguire ME, Becker LA, Crouch MLV, Fang FC. The phage shock protein PspA facilitates divalent metal transport and is required for virulence of *Salmonella enterica* sv. Typhimurium. Mol Microbiol. 2010; 78:669–685. [PubMed: 20807201]

Katayama A, Tsujii A, Wada A, Nishino T, Ishihama A. Systematic search for zinc-binding proteins in *Escherichia coli*. Eur J Biochem. 2002; 269:2403–2413. [PubMed: 11985624]

Kehl-Fie TE, Skaar EP. Nutritional immunity beyond iron: a role for manganese and zinc. Curr Opin Chem Biol. 2010; 14:218–224. [PubMed: 20015678]

Kim S, Watanabe K, Shirahata T, Watarai M. Zinc uptake system (*znuA* locus) of *Brucella abortus* is essential for intracellular survival and virulence in mice. J Vet Med Sci. 2004; 66:1059–1063. [PubMed: 15472468]

Kingsley RA, Reissbrodt R, Rabsch W, Ketley JM, Tsolis RM, Everest P, et al. Ferrioxamine-mediated iron(III) utilization by *Salmonella enterica*. Appl Environ Microbiol. 1999; 65:1610–1618. [PubMed: 10103258]

Kobayashi S, Hidaka S, Kawamura Y, Ozaki M, Hayase Y. Micacocidin A, B and C, novel antimycoplasma agents from *Pseudomonas* sp. I. taxonomy, fermentation, isolation, physico-chemical properties and biological activities. J Antibiot (Tokyo). 1998a; 51:323–327. [PubMed: 9589068]

Kobayashi S, Ikenishi Y, Takinami Y, Takema M, Sun WY, Ino A, Hayase Y. Preparation and antimicrobial activity of micacocidin. J Antibiot (Tokyo). 2000; 53:532–539. [PubMed: 10908118]

Kobayashi S, Nakai H, Ikenishi Y, Sun WY, Ozaki M, Hayase Y, Takeda R. Micacocidin A, B and C, novel antimycoplasma agents from *Pseudomonas* sp. II. Structure elucidation. J Antibiot (Tokyo). 1998b; 51:328–332. [PubMed: 9589069]

Kreutzer MF, Kage H, Gebhardt P, Wackler B, Saluz HP, Hoffmeister D, Nett M. Biosynthesis of a complex yersiniabactin-like natural product via the *mic* Locus in phytopathogen *Ralstonia solanacearum*. Appl Environ Microbiol. 2011; 77:6117–6124. [PubMed: 21724891]

Kumar P, Sannigrahi S, Tzeng YL. The *Neisseria meningitidis* ZnuD zinc receptor contributes to interactions with epithelial cells and supports heme utilization when expressed in *Escherichia coli*. Infect Immun. 2012; 80:657–667. [PubMed: 22083713]

Lathem WW, Price PA, Miller VL, Goldman WE. A plasminogen-activating protease specifically controls the development of primary pneumonic plague. Science. 2007; 315:509–513. [PubMed: 17255510]

Leach LH, Morris JC, Lewis TA. The role of the siderophore pyridine-2,6-bis (thiocarboxylic acid) (PDTC) in zinc utilization by *Pseudomonas putida* DSM 3601. BioMetals. 2007; 20:717–726. [PubMed: 17066327]

Lewis DA, Klesney-Tait J, Lumbley SR, Ward CK, Latimer JL, Ison CA, Hansen EJ. Identification of the *znuA*-encoded periplasmic zinc transport protein of *Haemophilus ducreyi*. Infect Immun. 1999; 67:5060–5068. [PubMed: 10496878]

Li Y, Qiu Y, Gao H, Guo Z, Han Y, Song Y, et al. Characterization of Zur-dependent genes and direct Zur targets in *Yersinia pestis*. BMC Microbiol. 2009; 9:128. [PubMed: 19552825]

Lim KHL, Jones CE, vanden Hoven RN, Edwards JL, Falsetta ML, Apicella MA, et al. Metal binding specificity of the MntABC permease of *Neisseria gonorrhoeae* and its influence on bacterial growth and interaction with cervical epithelial cells. Infect Immun. 2008; 76:3569–3576. [PubMed: 18426887]

Liu, Janet Z.; Jellbauer, S.; Poe, AJ.; Ton, V.; Pesciaroli, M.; Kehl-Fie, TE., et al. Zinc sequestration by the neutrophil protein calprotectin enhances *Salmonella* growth in the inflamed gut. Cell Host Microbe. 2012; 11:227–239. [PubMed: 22423963]

Liu M, Yan M, Liu L, Chen S. Characterization of a novel zinc transporter ZnuA acquired by *Vibrio parahaemolyticus* through horizontal gene transfer. Front Cell Infect Microbiol. 2013; 3:61. [PubMed: 24133656]

Liuzzi JP, Lichten LA, Rivera S, Blanchard RK, Aydemir TB, Knutson MD, et al. Interleukin-6 regulates the zinc transporter Zip14 in liver and contributes to the hypozincemia of the acute-phase response. Proc Natl Acad Sci U S A. 2005; 102:6843–6848. [PubMed: 15863613]

Lloubès R, Goemaere E, Zhang X, Cascales E, D D. Energetics of colicin import revealed by genetic cross-complementation between the Tol and Ton systems. Biochem Soc Trans. 2012; 40:1480–1485. [PubMed: 23176502]

Ma Z, Faulkner MJ, Helmann JD. Origins of specificity and cross-talk in metal ion sensing by *Bacillus subtilis* Fur. Mol Microbiol. 2012; 86:1144–1155. [PubMed: 23057863]

Michel L, Bachelard A, Reimmann C. Ferripyochelin uptake genes are involved in pyochelin-mediated signalling in *Pseudomonas aeruginosa*. Microbiology. 2007; 153:1508–1518. [PubMed: 17464065]

Miethke M, Marahiel MA. Siderophore-based iron acquisition and pathogen control. Microbiol Mol Biol Rev. 2007; 71:413–451. [PubMed: 17804665]

Miller DA, Luo L, Hillson N, Keating TA, Walsh CT. Yersiniabactin synthetase: a four-protein assembly line producing the nonribosomal peptide/polyketide hybrid siderophore of *Yersinia pestis*. Chem Biol. 2002; 9:333–449. [PubMed: 11927258]

Miller, JH. A Short Course in Bacterial Genetics A Laboratory Manual and Handbook for Escherichia coli and Related Bacteria. Cold Spring Harbor Laboratory Press; Cold Spring Harbor, N. Y: 1992.

Miller MC, DeMoll E. Extraction, purification, and Identification of Yersiniabactin, the siderophore of *Yersinia pestis*. Curr Prot Microbiol. 2011; 23:5B.3.1–5B.3.22.

Miller MC, Fetherston JD, Pickett CL, Bobrov AG, Weaver RH, DeMoll E, Perry RD. Reduced synthesis of the Ybt siderophore or production of aberrant Ybt-like molecules activates transcription of yersiniabactin genes in *Yersinia* pestis. Microbiology. 2010; 156:2226–2238. [PubMed: 20413552]

Mills SA, Marletta MA. Metal binding characteristics and role of iron oxidation in the ferric uptake regulator from Escherichia coli. Biochemistry. 2005; 44:13553–13559. [PubMed: 16216078]

Murphy TF, Brauer AL, Kirkham C, Johnson A, Koszelak-Rosenblum M, Malkowski MG. Role of the zinc uptake ABC transporter of *Moraxella catarrhalis* in persistence in the respiratory tract. Infect Immun. 2013; 81:3406–3413. [PubMed: 23817618]

Nakai H, Kobayashi S, Ozaki M, Hayase Y, Takeda R. Micacocidin A. Acta Crystallogr. 1999; C55:54–56.

Napolitano M, Rubio MÁ, Santamaría-Gómez J, Olmedo-Verd E, Robinson NJ, Luque I. Characterization of the response to zinc deficiency in the cyanobacterium *Anabaena* sp. Strain PCC 7120. J Bacteriol. 2012; 194:2426–2436. [PubMed: 22389488]

Nielubowicz GR, Smith SN, Mobley HLT. Zinc uptake contributes to motility and provides a competitive advantage to *Proteus mirabilis* during experimental urinary tract infection. Infect Immun. 2010; 78:2823–2833. [PubMed: 20385754]

Ó Cuív P, Clarke P, Lynch D, O'Connell M. Identification of *rhtX* and *fptX*, novel genes encoding proteins that show homology and function in the utilization of the siderophores rhizobactin 1021 by *Sinorhizobium meliloti* and pyochelin by *Pseudomonas aeruginosa*, respectively. J Bacteriol. 2004; 186:2996–3005. [PubMed: 15126460]

Perry RD, Abney J, Mier I Jr, Lee Y, Bearden SW, Fetherston JD. Regulation of the *Yersinia pestis* Yfe and Ybt iron transport systems. Adv Exp Med Biol. 2003a; 529:275–283. [PubMed: 12756771]

Perry RD, Balbo PB, Jones HA, Fetherston JD, DeMoll E. Yersiniabactin from *Yersinia pestis*: biochemical characterization of the siderophore and its role in iron transport and regulation. Microbiology. 1999; 145:1181–1190. [PubMed: 10376834]

Perry RD, Bobrov AG, Kirillina O, Rhodes ER, Actis LA, Fetherston JD. *Yersinia pestis* transition metal divalent cation transporters. Adv Exp Med Biol. 2012; 954:267–279. [PubMed: 22782773]

Perry RD, Fetherston JD. *Yersinia pestis* - etiologic agent of plague. Clin Microbiol Rev. 1997; 10:35–66. [PubMed: 8993858]

Perry, RD.; Fetherston, JD. Iron and heme uptake systems. In: Carniel, E.; Hinnebusch, BJ., editors. *Yersinia* Molecular and Cellular Biology. Norfolk, U.K.: Horizon Bioscience; 2004. p. 257-283.

Perry RD, Fetherston JD. Yersiniabactin iron uptake: mechanisms and role in *Yersinia pestis* pathogenesis. Microbes Infect. 2011; 13:808–817. [PubMed: 21609780]

Perry RD, Shah J, Bearden SW, Thompson JM, Fetherston JD. *Yersinia pestis* TonB: role in iron, heme and hemoprotein utilization. Infect Immun. 2003b; 71:4159–4162. [PubMed: 12819108]

Perry RD, Straley SC, Fetherston JD, Rose DJ, Gregor J, Blattner FR. DNA sequencing and analysis of the low-Ca^{2+}-response plasmid pCD1 of *Yersinia pestis* KIM5. Infect Immun. 1998; 66:4611–4623. [PubMed: 9746557]

Petrarca P, Ammendola S, Pasquali P, Battistoni A. The Zur-regulated ZinT protein is an auxiliary component of the high-affinity ZnuABC zinc transporter that facilitates metal recruitment during severe zinc shortage. J Bacteriol. 2010; 192:1553–1564. [PubMed: 20097857]

Plumptre CD, Eijkelkamp BA, Morey JR, Behr F, Couñago RM, Ogunniyi AD, et al. AdcA and AdcAII employ distinct zinc acquisition mechanisms and contribute additively to zinc homeostasis in *Streptococcus pneumoniae*. Mol Microbiol. 2014; 91:834–851. [PubMed: 24428621]

Rahuel-Claremont, S.; Dunn, MF. The biological chemistry of zinc. In: Rainsford, KD.; Milanino, R.; Sorenson, RJ.; Velo, GP., editors. Copper and Zinc in Inflammatory and Degenerative Diseases. Kluwer Academic Publisher; 1998. p. 47-59.

Ramakrishnan G, Meeker A, Dragulev B. *fslE* is necessary for siderophore-mediated iron acquisition in *Francisella tularensis* Schu S4. J Bacteriol. 2008; 190:5353–5361. [PubMed: 18539739]

Ramakrishnan G, Sen B, Johnson R. Paralogous outer membrane proteins mediate uptake of different forms of iron and synergistically govern virulence in *Francisella tularensis* tularensis. J Biol Chem. 2012; 287:25191–25202. [PubMed: 22661710]

Reed LJ, Muench H. A simple method for estimating fifty percent endpoints. Am J Hyg. 1938; 27:493–497.

Rink L, Haase H. Zinc homeostasis and immunity. Trends Immunol. 2007; 28:1–4. [PubMed: 17126599]

Rosadini CV, Gawronski JD, Raimunda D, Argüello JM, Akerley BJ. A novel zinc binding system, ZevAB, is critical for survival of nontypeable *Haemophilus influenzae* in a murine lung infection model. Infect Immun. 2011; 79:3366–3376. [PubMed: 21576338]

Sabri M, Houle S, Dozois CM. Roles of the extraintestinal pathogenic *Escherichia coli* ZnuACB and ZupT zinc transporters during urinary tract infection. Infect Immun. 2009; 77:1155–1164. [PubMed: 19103764]

Schaible UE, Kaufmann SHE. Iron and microbial infection. Nat Rev Microbiol. 2004; 2:946–953. [PubMed: 15550940]

Schalk IJ, Guillon L. Pyoverdine biosynthesis and secretion in *Pseudomonas aeruginosa*: implications for metal homeostasis. Environ Microbiol. 2013; 15:1661–1673. [PubMed: 23126435]

Schalk IJ, Hannauer M, Braud A. New roles for bacterial siderophores in metal transport and tolerance. Environ Microbiol. 2011; 13:2844–2854. [PubMed: 21883800]

Sebbane F, Jarrett C, Gardner D, Long D, Hinnebusch BJ. Role of the *Yersinia pestis* yersiniabactin iron acquisition system in the incidence of flea-borne plague. PLoS ONE. 2010; 5:e14379. [PubMed: 21179420]

Sebbane F, Jarrett CO, Gardner D, Long D, Hinnebusch BJ. Role of the *Yersinia pestis* plasminogen activator in the incidence of distinct septicemic and bubonic forms of flea-borne plague. Proc Natl Acad Sci U S A. 2006; 103:5526–5530. [PubMed: 16567636]

Sebbane F, Mandrand-Berthelot MA, Simonet M. Genes encoding specific nickel transport systems flank the chromosomal urease locus of pathogenic Yersiniae. J Bacteriol. 2002; 184:5706–5713. [PubMed: 12270829]

Sheikh MA, Taylor GL. Crystal structure of the *Vibrio cholerae* ferric uptake regulator (Fur) reveals insights into metal co-ordination. Mol Microbiol. 2009; 72:1208–1220. [PubMed: 19400801]

Sohnle PG, Hunter Michael J, Hahn B, Chazin Walter J. Zinc reversible antimicrobial activity of recombinant calprotectin (migration inhibitory factor - related proteins 8 and 14). J Infect Dis. 2000; 182:1272–1275. [PubMed: 10979933]

Stork M, Bos MP, Jongerius I, de Kok N, Schilders I, Weynants VE, et al. An outer membrane receptor of *Neisseria meningitidis* involved in zinc acquisition with vaccine potential. PLoS Pathog. 2010; 6:e1000969. [PubMed: 20617164]

Stork M, Grijpstra J, Bos MP, Mañas Torres C, Devos N, Poolman JT, et al. Zinc piracy as a mechanism of *Neisseria meningitidis* for evasion of nutritional immunity. PLoS Pathog. 2013; 9:e1003733. [PubMed: 24204275]

Surgalla MJ, Beesley ED. Congo red-agar plating medium for detecting pigmentation in *Pasteurella pestis*. Appl Microbiol. 1969; 18:834–837. [PubMed: 5370459]

Une T, Brubaker RR. In vivo comparison of avirulent Vwa$^-$ and Pgm$^-$ or Pst^r phenotypes of yersiniae. Infect Immun. 1984; 43:895–900. [PubMed: 6365786]

Vallee BL, Falchuk KH. The biochemical basis of zinc physiology. Physiol Rev. 1993; 73:79–118. [PubMed: 8419966]

Weinberg ED. Infectious diseases influenced by trace element enviroment. Ann NY Acad Sci. 1972; 199:274–284. [PubMed: 4506512]

Weston BF, Brenot A, Caparon MG. The metal homeostasis protein, Lsp, of *Streptococcus pyogenes* is necessary for acquisition of zinc and virulence. Infect Immun. 2009; 77:2840–2848. [PubMed: 19398546]

Yang X, Becker T, Walters N, Pascual DW. Deletion of *znuA* virulence factor attenuates *Brucella abortus* and confers protection against wild-type challenge. Infect Immun. 2006; 74:3874–3879. [PubMed: 16790759]

Youard Z, Wenner N, Reimmann C. Iron acquisition with the natural siderophore enantiomers pyochelin and enantio-pyochelin in *Pseudomonas* species. BioMetals. 2011; 24:513–522. [PubMed: 21188474]

Zhao B, Moody SC, Hider RC, Lei L, Kelly SL, Waterman MR, Lamb DC. Structural analysis of cytochrome P450 105N1 involved in the biosynthesis of the zincophore, coelibactin. Int J Mol Sci. 2012; 13:8500–8513. [PubMed: 22942716]

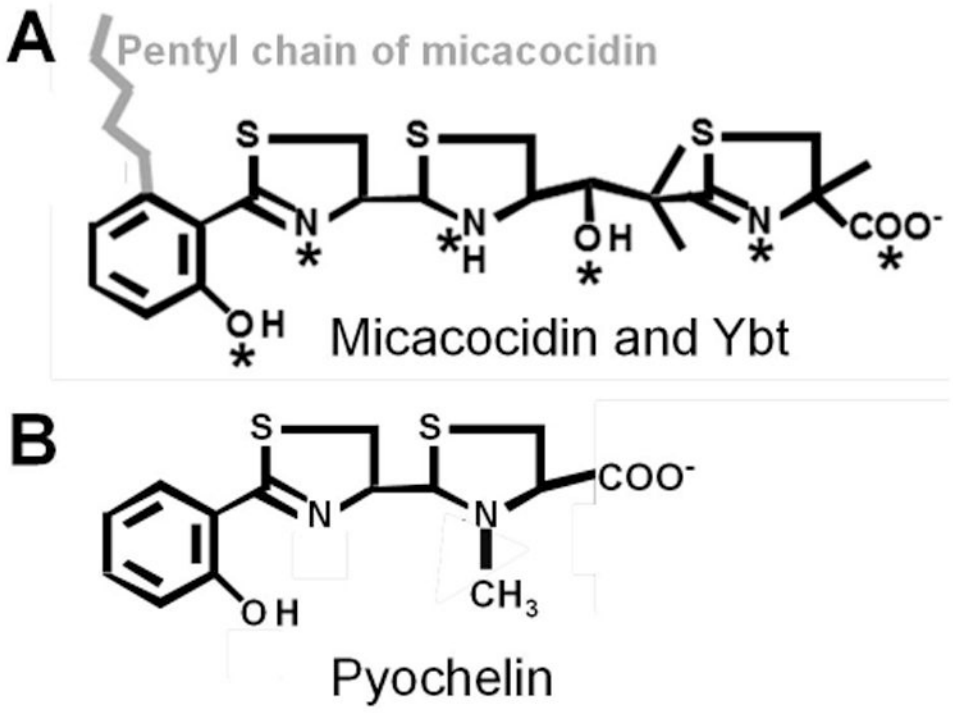

Fig. 1.

The structures of Ybt, micacocidin (A) and pyochelin (B). The asterisks indicate Fe^{3+} chelation sites in Ybt. The pentyl chain (in grey) of micacocidin is the only structural difference with Ybt (A). Pyochelin (B) lacks the malonyl linker and second thiazoline ring present in YbtA (A).

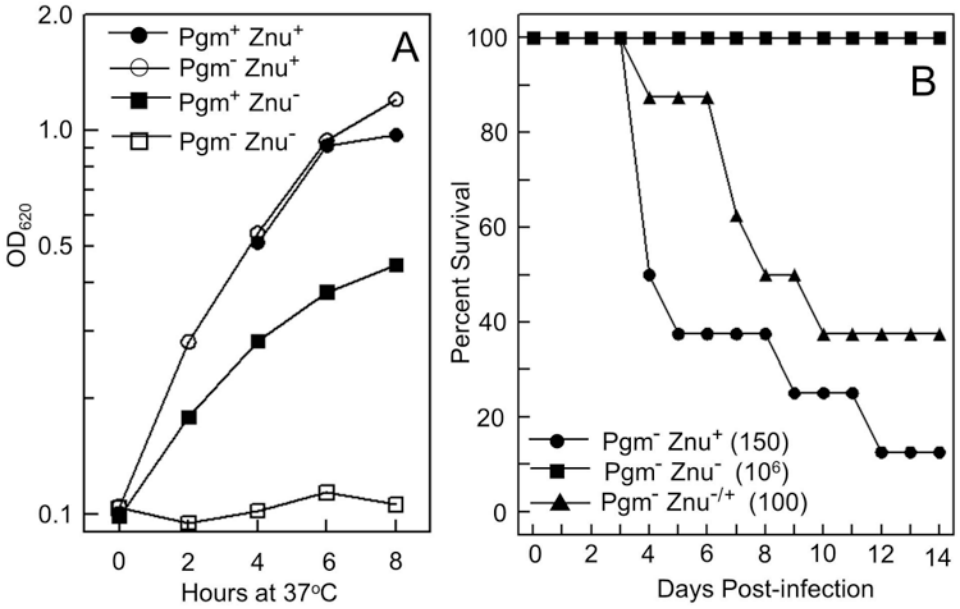

Fig. 2.

Growth and virulence of a *Y. pestis* Pgm$^-$ Znu$^-$ mutant. A. Cells were grown at 37°C in cPMH2 supplemented with 0.6 μM $ZnCl_2$; strains: KIM6+ (Pgm$^+$ Znu$^+$); KIM6 (Pgm$^-$ [Δ*pgm*] Znu$^+$); KIM6-2077+ (Pgm$^+$ Znu$^-$ [Δ*znuB*C]); KIM6-2077 (Pgm$^-$ [Δ*pgm*] Znu$^-$ [Δ*znuB*C]). Growth curves shown are from one experiment that is representative of two or more independent experiments. B. Average time-to-death (percent survival) analyses for two independent septicemic *Y. pestis* infections. Strains: KIM5-2077(pCD1Ap) (Pgm$^-$ [Δ*pgm*] Znu$^-$ [Δ*znuB*C]); KIM5(pCD1Ap) (Pgm$^-$ [Δ*pgm*] Znu$^+$); KIM5-2077.10(pCD1Ap) (Pgm$^-$ [Δ*pgm*] Znu$^{-/+}$ [Δ*znuB*C/*znuABC*$^+$]). The average infectious doses are indicated in parentheses.

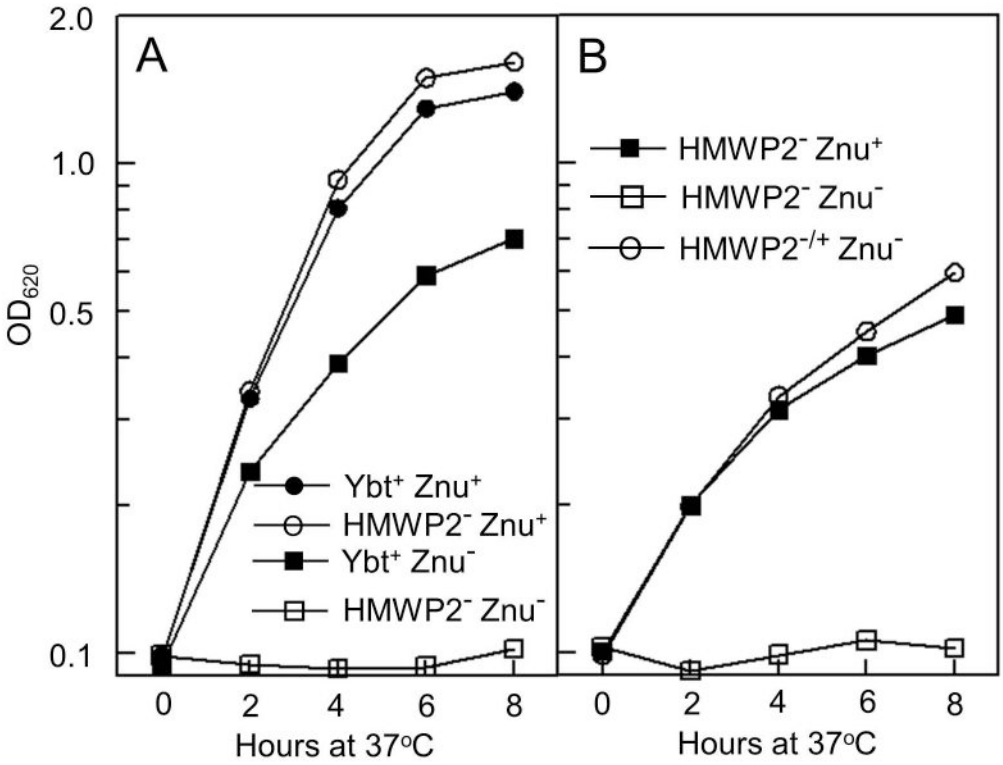

Fig. 3.

The *Y. pestis* HMWP2^{-} Znu^{-} mutant has a severe growth defect at 37°C in cPMH2 supplemented with 0.6 μM $ZnCl_2$ and 1.0 μM $FeCl_3$. A: Strains – KIM6+ (Ybt^{+} Znu^{+}); KIM6-2046.1 (HMWP2^{-} [*irp2*::*kan*] Znu^{+}); KIM6-2077+ (Ybt^{+} Znu^{-} [Δ*znuBC*]); KIM6-2077.7 (HMWP2^{-} [*irp2*::*kan*] Znu^{-} [Δ*znuBC*]). B: strains – KIM6-2046.3(pBGL2) (HMWP2^{-} [Δ*irp2*] Znu^{+}); KIM6-2077.8 (Δ*irp2* Δ*znuBC*) carrying pBGL2 (HMWP2^{-} Znu^{-}) or pIrp2 (HMWP2$^{-/+}$ Znu^{-}). An *irp2* mutant cannot express the Ybt synthetase HMWP2 and thus cannot synthesize the Ybt siderophore (Perry and Fetherston, 2011). To complement the in-frame Δ*irp2* mutation (KIM6-2077.8), the WT *irp2* gene with its native promoter was cloned into the pBGL2 vector plasmid generating pIrp2. Growth curves shown are from one experiment that is representative of two or more independent experiments.

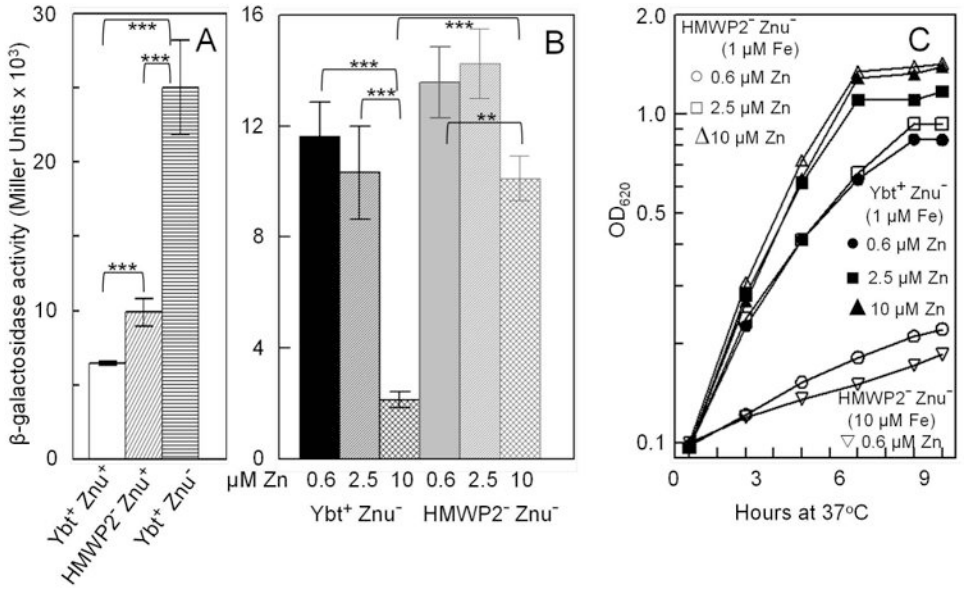

Fig. 4.

An *irp2* mutation in *Y. pestis* results in lower intracellular Zn^{2+} levels (A and B) and increases the concentration of exogenous Zn^{2+} required to stimulate growth (C). The β-galactosidase activities shown (A and B) are averages (with standard deviations) of replicate samples from two independent cultures. Statistical significances were calculated using the Student's two tailed t-test; p = <0.001 - ***; p = < 0.005 - **. Growth curves (C) shown are from one experiment that is representative of two or more independent experiments. Strains were grown in cPMH2 at 37°C unsupplemented (A) or with increasing levels of $ZnCl_2$ (B and C). cPMH was also supplemented with 1.0 μM $FeCl_3$ (B) or indicated $FeCl_3$ concentrations (C). Strains: KIM6+ (Ybt$^+$ Znu$^+$); KIM6-2046.1 (HMWP2$^-$ [*irp2::kan*] Znu$^+$); KIM6-2077+ (Ybt$^+$ Znu$^-$ [Δ*znuBC*]); KIM6-2077.7 (HMWP2$^-$ [*irp2::kan*] Znu$^-$ [Δ*znuBC*]). In A and B, all strains carry pEUZnu1 which encodes the *znuA::lacZ* transcriptional reporter.

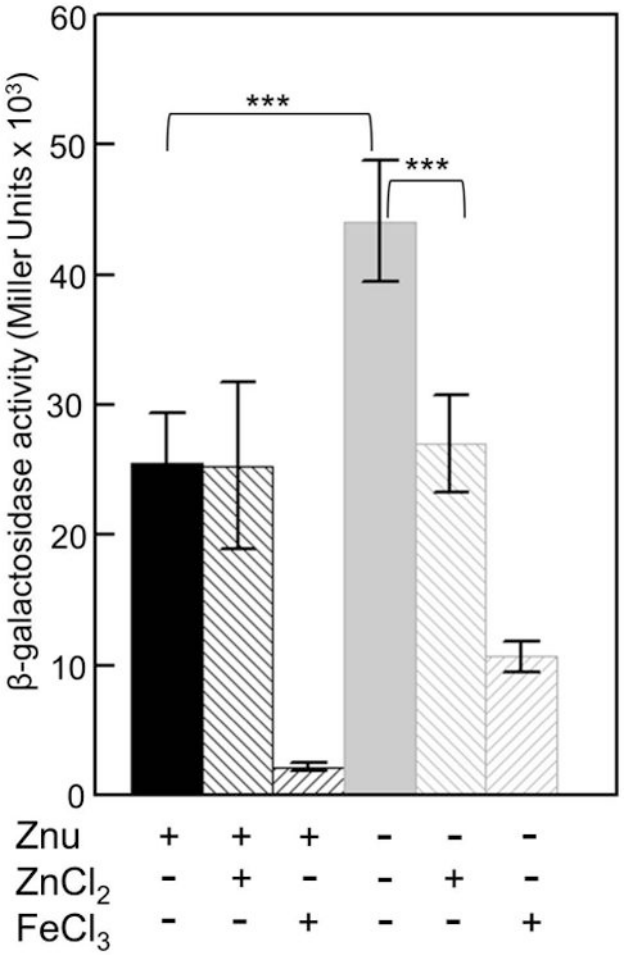

Fig. 5.

Transcription from the *irp2* promoter is affected by Zn^{2+}. The β-galactosidase activities from the *irp2*::*lacZ* transcriptional reporter carried by KIM6+ (Znu +) or KIM6-2077+ (Znu -) are averages (with standard deviations) of replicate samples from two independent cultures. Strains were grown in cPMH2 at 37°C unsupplemented or with $ZnCl_2$ or $FeCl_3$ added to 10 μM. Statistical significances were calculated using the Student's two tailed t-test; p = <0.001 - ***. As previously demonstrated (Perry *et al.*, 2003a), transcription from the *irp2*::*lacZ* reporter in both strains was repressed by $FeCl_3$ supplementation (p = $<3 \times 10^{-7}$; not shown on the graph for clarity).

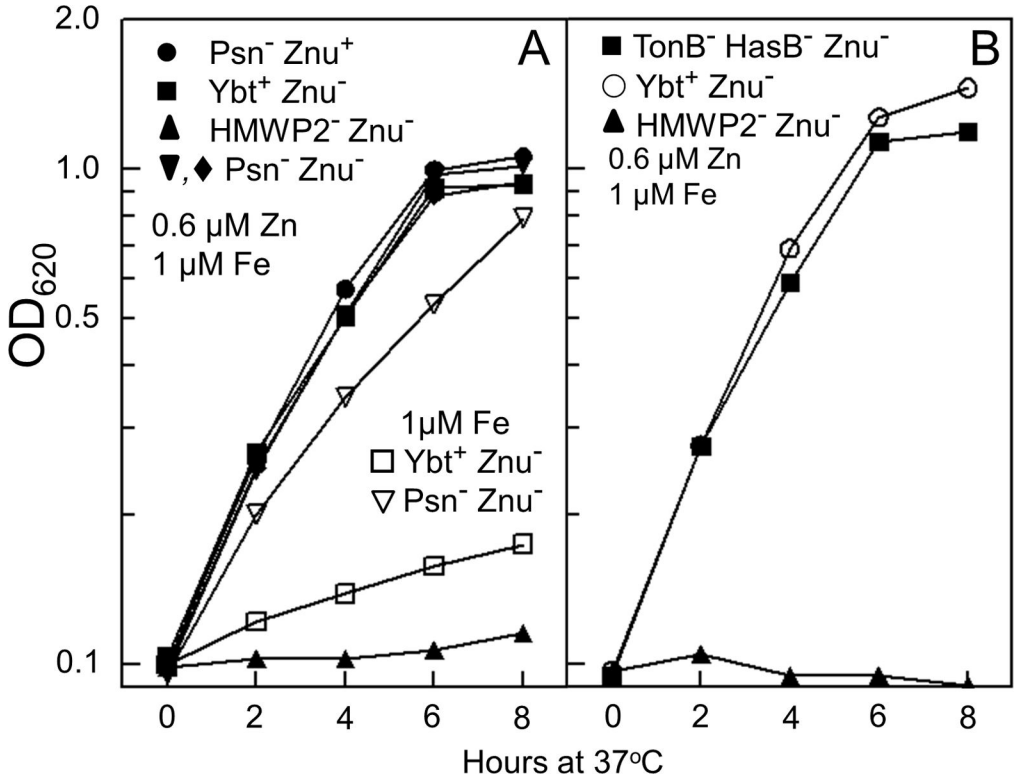

Fig. 6.

Ybt-dependent Zn^{2+} acquisition does not require the OM Ybt receptor Psn or any other TonB-dependent OM receptor. Cells were grown at 37°C in cPMH2 supplemented with 0.6 μM $ZnCl_2$ and 1.0 μM $FeCl_3$ or 1.0 μM $FeCl_3$ alone. Strains: KIM6-2045.1 (Psn^- [Δ*psn*] Znu^+); KIM6-2077+ (Ybt^+ Znu^- [Δ*znuBC*]); KIM6-2077.7 ($HMWP2^-$ [*irp2::kan*] Znu^- [Δ*znuBC*]); KIM6-2077.12+ (Znu^- [Δ*znuBC*] $TonB^-$[*tonB::kan*] $HasB^-$ [Δ*hasB*]); Psn^- Znu^- (KIM6-2077.9 [*psn::kan* Δ*znuBC*], ▼ and KIM6-2077.14 [Δ*psn* Δ*znuBC*];◆). Psn is the OM receptor for Ybt and HasB is a second TonB-like protein in *Y. pestis* (Perry and Fetherston, 2011; Perry *et al.*, 2003b). Growth curves shown are from one experiment that is representative of two or more independent experiments.

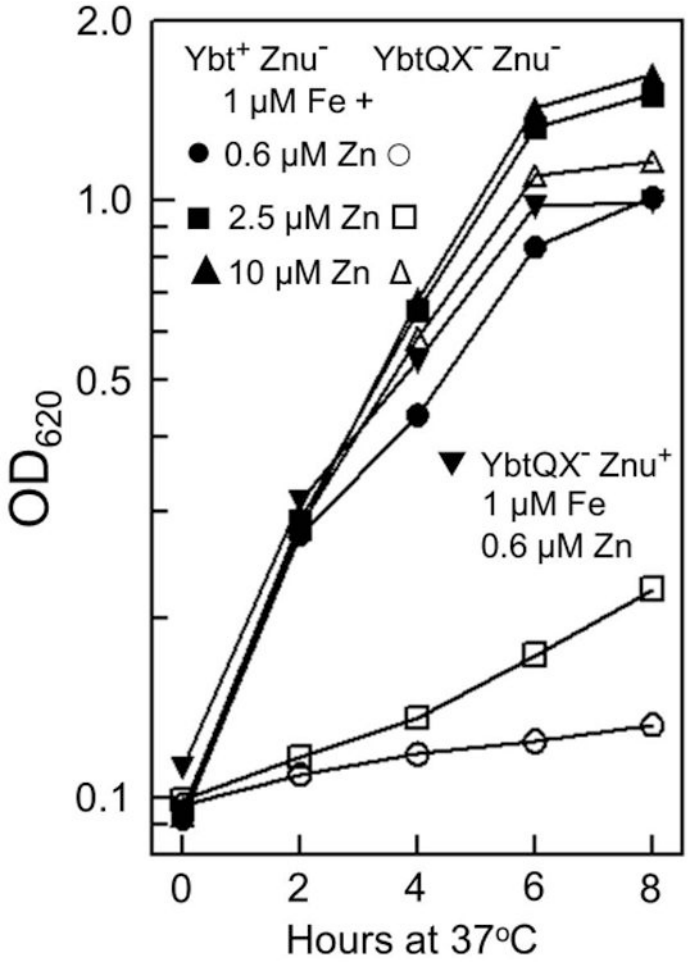

Fig. 7.

A YbtQX$^-$ Znu$^-$ mutant (open symbols) has a severe growth defect and requires additional Zn^{2+} supplementation to restore growth, compared to single Znu$^-$ and YbtQX$^-$ mutants (closed symbols). Cells were grown at 37°C in cPMH2 with 1.0 μM $FeCl_3$ and increasing levels of $ZnCl_2$. Strains: KIM6-2066 (YbtQX$^-$ [Δ*ybtQX*]); KIM6-2077+ (Znu$^-$ [Δ*znuBC*]); KIM6-2077.13 (YbtQX$^-$ [Δ*ybtQX*] Znu$^-$ [Δ*znuBC*]). YbtQ, but not YbtX, is part of the IM ABC transporter (YbtPQ) required for the use of Fe^{3+} from Ybt (Perry and Fetherston, 2011). Growth curves shown are from one experiment that is representative of two or more independent experiments.

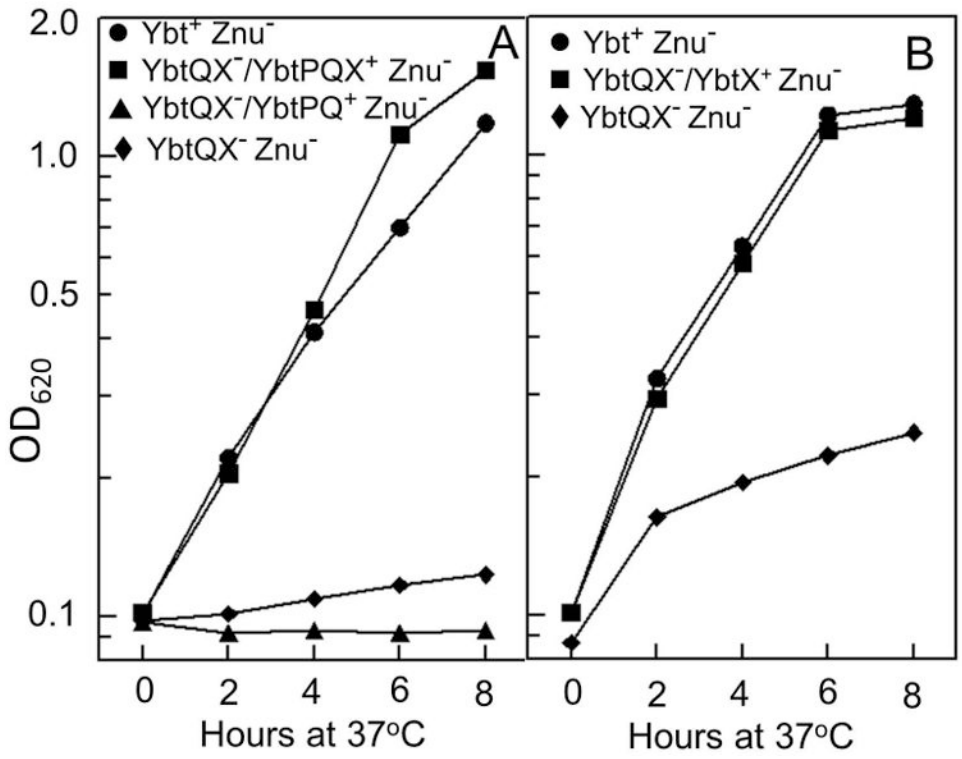

Fig. 8.

YbtX is required for Ybt-dependent Zn^{2+} uptake. Cells were grown at 37°C in cPMH2 with 1.0 μM $FeCl_3$ and 0.6 μM $ZnCl_2$. A. The growth of KIM6-2077.13 (YbtQX$^-$ [Δ*ybtQX*] Znu$^-$ [Δ*znuBC*] is restored when carrying pYbtPQX, which expresses *ybtPQX*$^+$ (YbtQX$^-$/YbtPQX$^+$) but not when carrying pYbtPQ, which expresses only *ybtPQ*$^+$ (YbtQX$^-$/YbtPQ$^+$). B. A plasmid (pYbtX) expressing only *ybtX*$^+$ restored the growth of KIM6-2077.13. KIM6-2077+ (Ybt$^+$ Znu$^-$ [Δ*znuBC*]) and strains carrying the vector plasmid pACYC184 were used as controls. Growth curves shown are from one experiment that is representative of two or more independent experiments.

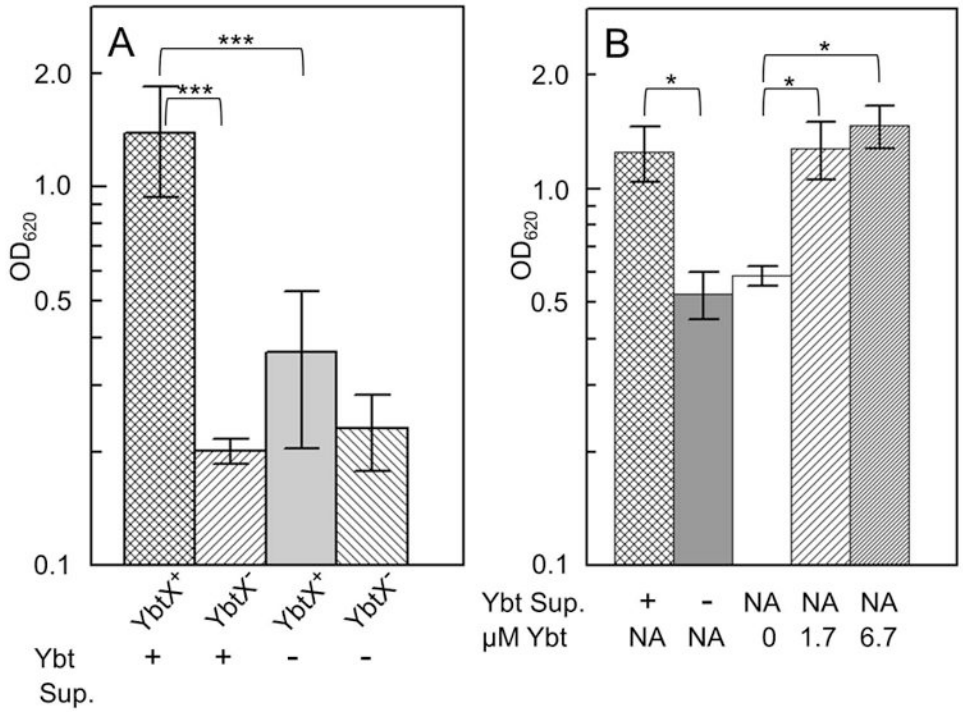

Fig. 9.

Addition of apo-Ybt or culture supernatants containing Ybt stimulates the growth of the Δ*znuBC* Δ*psn irp2*::*kan* mutant. A. After acclimation to growth at 37°C in cPMH2 supplemented with 0.6 μM $ZnCl_2$ and 1.0 μM $FeCl_3$, cultures were then back diluted to an OD_{620} of ~0.1 in a 1:1 mixture of the same medium with culture supernatants. B. Alternatively, similarly grown cultures of the Δ*znuBC* Δ*psn irp2*::*kan* mutant were back diluted to an OD_{620} of 0.1 and incubated with apo-Ybt (μM Ybt) or ethanol solvent (0 μM Ybt). Culture optical densities were measured after overnight incubation at 37°C. Strains KIM6-2077.18 (Δ*znuBC* Δ*psn irp2*::*kan*; labeled $YbtX^+$) and KIM6-2077.19 (Δ*znuBC* Δ*psn irp2*::*kan* Δ*ybtX*; labeled $YbtX^-$) were tested for growth with supernatants from KIM6+ (Ybt +) and KIM6-2046.1 (*irp2*::*kan;* Ybt -) (Panel A and B) or apo-Ybt (Panel B). Addition of apo-Ybt to a final concentration of 1.7 μM is equivalent to the Ybt present in cultures with at a 1:1 mixture with supernatant from KIM6+. NA – not applicable. Data presented for the $YbtX^+$ strain are averages from 10 independent experiments with 6 independent culture supernatants (panel A) or 3 independent experiments (panel B). Data presented for the $YbtX^-$ strain are averages from two or more independent experiments supplemented with 2 independent culture supernatants (panel A). Error bars represent standard deviations while asterisks with brackets indicate statistical significances calculated using the Student's two tailed t-test (p = <0.001 - ***; p = <0.05 - *).

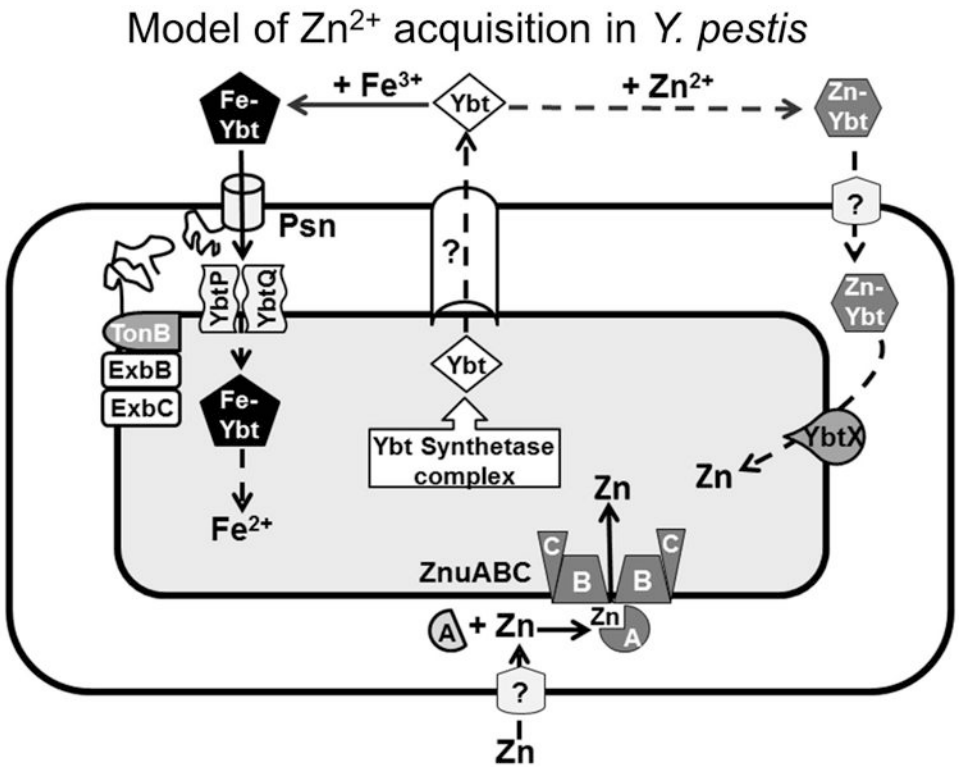

Fig. 10.

A proposed model of Zn^{2+} uptake in *Y. pestis*. Fe^{3+} uptake via the Ybt system as well as Zn^{2+} uptake is shown. Dashed arrows represent putative steps. Our results suggest passage through both the OM and IM when exogenous Ybt is supplied.

Table 1
Virulence of *Y. pestis* strains in a mouse model of septicemic plague

Strain or genotype[a]	LD_{50} values[b]	Virulence loss
Δ*pgm*	<6 ± 2.8 (<8; 4)	--
Δ*pgm* Δ*znu*	$5.7 \times 10^6 \pm 4.2 \times 10^6$	$>9.5 \times 10^5$-fold
Δ*pgm* Δ*znuBC att*Tn*7*::*znuABC*$^+$	<10; >101; 25	--
Wild type	<14 ± 1.4 (<13; <15)	--
Δ*znu*	∼11 ± 5 (<10; >16; <8; <18)	none
irp2::*kan*	∼ 48 (<11; 84.5)	none
irp2 Δ*znu*	$\sim 6.0 \times 10^6 \pm 3.5 \times 10^6$ (5.1×10^6; 2.7×10^6; 5.4×10^6; $>1.1 \times 10^7$)	$>4.3 \times 10^5$-fold
Δ*psn*::*kan*	<14	none
Δ*psn*::*kan* Δ*znuBC*	∼40 ± 14 (30; <50)	none

[a] Strains: Δ*pgm* – KIM5(pCD1Ap); Δ*pgm* Δ*znu* – KIM5-2077(pCD1Ap) [Δ*pgm* Δ*znuBC*] and KIM5-2197(pCD1Ap) [Δ*pgm* Δ*znuA*]; Δ*pgm* Δ*znuBC att*Tn*7*::*znuABC* – KIM5-2077.10(pCD1Ap); wild type - KIM5(pCD1Ap)+; Δ*znu* – KIM5-2077(pCD1Ap)+ [Δ*znuBC*] and KIM5-2197(pCD1Ap)+ [Δ*znuA*]; *irp2*::*kan* – KIM5-2046.1(pCD1Ap); *irp2* Δ*znu* – KIM5-2077.7(pCD1Ap) [*irp2*::*kan* Δ*znuBC*], KIM5-2077.8(pCD1Ap) [Δ*irp2* Δ*znuBC*] and KIM5-2197.1(pCD1Ap) [Δ*irp2* Δ*znuA*]; Δ*psn*::*kan* – KIM5-2045.6(pCD1Ap); Δ*psn*::*kan* Δ*znuBC* – KIM5-2077.9(pCD1Ap). In all backgrounds tested, an in-frame Δ*znuA* mutation and the Δ*znuBC* mutation caused similar LD_{50}s. In addition, *irp2*::*kan* and Δ*irp2* mutations in all backgrounds tested yielded similar LD_{50}s. These LD_{50}s were combined and genotypes for these strains are listed in the table as Δ*znu*, Δ*pgm* Δ*znu*, and *irp2* Δ*znu*.

[b] Where the LD_{50} was lower than the lowest dose of the trial (e.g., <8) or higher than the highest dose (e.g., >16), these doses and the calculated LD_{50}s are given in parentheses (e.g., <8; 4) and were used in calculating the mean LD_{50}. The means ± standard deviations from two to four separate trials are given, except for the Δ*pgm* Δ*znuBC att*Tn*7*::*znuABC*$^+$ strain were the LD_{50}s of three separate trials are listed.